

Instituto Tecnológico y de Estudios Superiores de Monterrey

Campus Monterrey

School of Engineering and Sciences



Development of a piezoelectric smart device with fiber meshes elaborated  
by Forcespinning™.

A thesis presented by

Renato Wenceslao Aguirre Corona

Submitted to the  
School of Engineering and Sciences  
in partial fulfillment of the requirements for the degree of

Master of Science

In

Nanotechnology

Monterrey Nuevo León, June 14<sup>th</sup>, 2022

## **Dedication**

I want to dedicate this work to that special person that was along the whole path of my master's degree, who was encouraging me and giving me her support, to never give up and made me believe in myself continuously. I will be thankful with her for the rest of my life.

I also want to dedicate this work, for my parents who were by my side giving me their infinite support and love.

To my sister, my accomplice in the most of my acts in life, who is always with me also giving me her support and love, listening to all my problems, and giving me advice.

To those loyal friends that believed in me.

## **Acknowledgements**

I would like to express my deepest gratitude to all those who have been by my side with me until the completion of this project, to Dr. Karina del Ángel, Dr. Nicolas Ulloa, Dr Juan Rodríguez, Dr. Cintya Soria, Dr. Oscar Martínez Romero, Dr. Daniel Olvera Trejo, MSc Ricardo Flores and MSc Emiliano Reséndiz.

I am so grateful for all the support, advice and care that was given to me by the Dr. Alex Elías Zúñiga, who was always encouraging me to believe in myself until the completion of this project.

I want to express my gratitude to the Tecnológico de Monterrey by all the support given to me and the scholarship, it is an honor to form part of this institution, and to the CONACyT for the living support that was given to me through my master program.

# **Development of a piezoelectric smart device with fiber meshes elaborated by Forcespinning™**

by

Renato Wenceslao Aguirre Corona

## **Abstract**

A novel approach was used in this thesis project. BaTiO<sub>3</sub> nanoparticles named as BTO nanoparticles were synthesized in the laboratory and commercial graphene named as G are used as fillers in Polyvinylidene Fluoride named as PVDF for the formation of polymeric meshes for the development of piezoelectric devices. Piezoelectric fiber meshes from different materials as: PVDF, BTO/PVDF, G/PVDF, BTO/G/PVDF are done varying the concentration of the fillers to evaluate the materials. The fiber meshes were fabricated in the Forcespinning™ technique and were characterized using different techniques.

Scanning Electron Microscopy was used to obtain the morphology and chemical composition by Energy Dispersive Spectroscopy(EDS), Fourier Transformed Infrared Spectroscopy (FTIR) was done for the identification of the phase composition of the material, Thermogravimetric Analysis allows the obtention of the maximum temperature of degradation to identify the materials with more thermal stability and X-ray Diffraction confirmed us the presence of the planes of the  $\beta$  phase in the fiber meshes and in the BTO the planes that are in concordance to the crystallographic card 96-150-7758. For the characterization of the piezoelectric devices an Impact tester was used with a multimeter to record the voltage generated by all the samples.

Where the mean maximum voltage generated for the A2 device is 35.77 V<sub>oc</sub>, the best device with only BTO as filler, while A3, A4, A6 and A7 samples are samples where G is used with a bad performance. The devices developed can be used for different applications as sensors or nanogenerators, showing a promising performance.

Piezoelectric devices are of interest by the generation of voltage from sources that were not used before, therefore producing energy from sustainable alternatives, offering an option for remote self-powered sensors.

## List of Figures

Figure 1. Piezoelectric phenomena .....	34
Figure 2. Piezoelectric Materials .....	38
Figure 3. PVDF molecular structure for $\alpha$ phase and $\beta$ phase .....	39
Figure 4. Piezoelectric nanofillers.....	40
Figure 5. Fabrication Techniques for Piezoelectric sensors.....	42
Figure 6. Forcespinning™ technique diagram.....	45
Figure 7. Diagram of synthesis of BTO. ....	51
Figure 8. Diagram of the fiber synthesis.....	54
Figure 9. Device design. ....	55
Figure 10. SEM image of BTO particles with a graph of the size of the particles.....	58
Figure 11. XRD Diffractogram of BTO.....	60
Figure 12. SEM images of the nanofibers for each composite with a graph for the representation of the mean diameter of the fibers. A1) PVDF, A2) BTO 15%/ PVDF, A3) G 0.05%/PVDF, A4) BTO 15%/G 0.05%/PVDF, A5) BTO 5%/PVDF, A6) G 0.15%/PVDF, A7) BTO 15%/G 0.15%/PVDF. ....	62
Figure 13. EDS images of the nanofibers for A5) BTO 5%/PVDF, we can observe the distribution of the material in the meshes of each element of the BTO, and a punctual test to observe the presence of the BTO in the meshes.....	63
Figure 14. EDS images of the nanofibers for A4) BTO 15%/G 0.05%/PVDF, we can observe the distribution of the material in the meshes of each element of the BTO, and a punctual test to observe the presence of the BTO in the meshes.....	63
Figure 15. EDS images of the nanofibers for A7: BTO 15%/G 0.15%/PVDF, we can observe the distribution of the material in the meshes of each element of the BTO, and a punctual test to observe the presence of the BTO in the meshes.....	64
Figure 16. FTIR spectra from all the composites and the raw material. A1) PVDF, A2) BTO 15%/ PVDF, A3) G 0.05%/PVDF, A4) BTO 15%/G 0.05%/PVDF, A5) BTO 5%/PVDF, A6) G 0.15%/PVDF, A7) BTO 15%/G 0.15%/PVDF. ....	66
Figure 17. TGA Thermograms from all the samples. A1) PVDF, A2) BTO 15%/ PVDF, A3) G 0.05%/PVDF, A4) BTO 15%/G 0.05%/PVDF, A5) BTO 5%/PVDF, A6) G 0.15%/PVDF, A7) BTO 15%/G 0.15%/PVDF. ....	69

Figure 18. TGA Derivatives of the thermograms from all the samples. A1) PVDF, A2) BTO 15%/PVDF, A3) G 0.05%/PVDF, A4) BTO 15%/G 0.05%/PVDF, A5) BTO 5%/PVDF, A6) G 0.15%/PVDF, A7) BTO 15%/G 0.15%/PVDF. ....	70
Figure 19. XRD Diffractogram of all the samples. A1) PVDF, A2) BTO 15%/ PVDF, A3) G 0.05%/PVDF, A4) BTO 15%/G 0.05%/PVDF, A5) BTO 5%/PVDF, A6) G 0.15%/PVDF, A7) BTO 15%/G 0.15%/PVDF. ....	73
Figure 20. Device distribution by voltage output. A1) PVDF, A2) BTO 15%/ PVDF, A3) G 0.05%/PVDF, A4) BTO 15%/G 0.05%/PVDF, A5) BTO 5%/PVDF, A6) G 0.15%/PVDF, A7) BTO 15%/G 0.15%/PVDF. ....	74
Figure 21. Boxplot of the voltage measured with the multimeter. A1) PVDF, A2) BTO 15%/PVDF, A3) G 0.05%/PVDF, A4) BTO 15%/G 0.05%/PVDF, A5) BTO 5%/PVDF, A6) G 0.15%/PVDF, A7) BTO 15%/G 0.15%/PVDF. ....	75
Figure 22. Electrical circuit for the piezoelectric coefficient. ....	78
Figure 23. Voltage generated at different positions for sample A2) BTO 15%/PVDF. Value of the force for each position P0 = 2.77N, P1 = 2.44 N, P2 = 2.27 N, P3 = 1.84 N, and P4 = 1.57 N ..	79
Figure 24. Shape for the signal obtained from the oscilloscope.....	80
Figure 25. Devices fabricated from the different composites. ....	81
Figure 26. Diagram of the measuring process for the obtention of the output voltage. ....	81

## List of Tables

Table 1. State of the art of Piezoelectric nanogenerators and Forcespinning™ sensors .....	19
Table 2. IoT five-layer Architecture.....	30
Table 3. Communication Architecture for Wearable Devices.....	32
Table 4. Preliminary tests parameters. ....	52
Table 5. Description of every solution that was used for the fabrication of piezoelectric sensors. .....	53
Table 6. Phase $\beta$ percentage calculations from FTIR spectra. ....	67
Table 7. Maximum degradation temperature.....	71
Table 8. Mean voltage produced by each device. ....	75
Table 9. Piezoelectric Sensitivity .....	76
Table 10. Piezoelectric Coefficient .....	77
Table 11. Piezoelectric devices comparison.....	83



## Contents

<b>Abstract</b>	<b>v</b>
<b>List of Figures</b>	<b>vi</b>
<b>List of Tables</b>	<b>vii</b>
1. Introduction.....	13
1.1 Motivation.....	17
1.2 Problem Statement and Context.....	18
1.3 State of the art.....	18
1.4 Objectives (General Purpose).....	27
1.4.1 Specific Objectives.....	27
1.5 Hypothesis.....	27
1.6 Scope.....	28
1.7 Dissertation.....	28
1.8 Solution Overview.....	29
2. Theoretical Aspects.....	30
2.1 Internet of Things.....	30
2.2 Smart Sensors.....	31
2.3 Communication Protocols.....	32
2.4 Piezoelectricity.....	33
2.5 Device Structures.....	35
2.6 Mode of Operation.....	36
2.7 Piezoelectric Materials.....	36
2.8 PVDF.....	38
2.9 Nanofillers.....	39
2.10 Solvents.....	41
2.11 Substrates.....	41
2.12 Fabrication Techniques.....	42
2.12.1 Electrospinning.....	43
2.12.2 Additive manufacturing.....	43
2.12.3 Spin Coating.....	43
2.12.4 Deposition.....	43

2.12.5 Hot Press.....	44
2.12.6 Forcespinning™ .....	44
2.13 Structures of Materials.....	45
2.14 Applications.....	46
2.12.1 Healthcare.....	46
2.12.2 Buildings and Infrastructure.....	47
2.12.3 Vehicles .....	48
2.12.4 Industry .....	48
3. Materials and Methods .....	50
3.1 Materials.....	50
3.2 Methodology for preparation of Barium Titanate .....	50
3.3 Solution preparation.....	52
3.5 Elaboration of fibers .....	54
3.6 Device Construction .....	55
3.7 Characterization.....	56
3.7.1 SEM Morphologic and Elemental distribution Characterization.....	56
3.7.2 FTIR Composition Characterization .....	56
3.7.3 TGA Thermal Characterization .....	56
3.7.4 XRD Structural Characterization.....	57
3.7.5 Piezoelectric Characterization.....	57
4. Results and Discussion .....	58
4.1 Barium Titanate Synthesis .....	58
4.2 Nanofiber Synthesis .....	61
4.2.1 Morphologic Characterization.....	61
4.2.2 FTIR Composition Characterization .....	65
4.2.3 Thermal Characterization.....	68
4.2.4 Structural characterization .....	72
4.2.5 Piezoelectric characterization.....	74
5. Conclusion.....	85
6. Future Work.....	87
Bibliography .....	88
Curriculum Vitae.....	96

# Chapter 1

## 1. Introduction

Actually, the development and usage of advanced materials for the miniaturization of electronics, helps in the creation of new electronic devices for different applications, these devices are in the scope of scientists by their novelty, some of them will take part in the internet of things (IoT) system where batteries are used to energize devices, but there is an effort in developing materials that can help to replace these batteries to reduce or eliminate the damage produced to the environment by using these sustainable alternatives <sup>1</sup>. The internet of things is a system where the communication from several devices that are in our environments, like sensors and actuators, is performed between themselves to fulfill a common objective <sup>1-4</sup>. The IoT system is divided into 5 different layers to achieve the interconnection between several devices, among them, the object layer is where the systems as sensors and actuators are involved <sup>5</sup>. Sensors are a cornerstone for this IoT system because through them, all the data can be collected and transmitted to perform other actions as the control of a system or the monitoring of signals <sup>6</sup>. The IoT technology is going to be present in several areas to make the exchange of communication more efficiently and easier, hence sensors will be needed in these areas too, for example in healthcare, buildings, vehicles, houses, personal devices, and industries <sup>1-3</sup>. Within the sensors for IoT, wearables for healthcare are experiencing an increment in demand and evolving to perform more actions and become smarter by the feasibility and the practicality that these sensors offer to this area <sup>7,8</sup>. Smart sensors in the healthcare area are used as wearables for the prevention, monitoring, and treatment of diseases; also, in this area, sensors can be classified depending on the working mechanism that the sensors use to obtain the information, like piezoelectric, resistive, capacitive, piezoresistive, piezothermal, and triboelectric <sup>7</sup>. Therefore, piezoelectric sensors are of main interest for their performance and due to the possibility of supplying energy to other electronic circuits and performing the function of a sensor.

Also, this type of technology allows the obtention of energy from natural energy resources, reducing the usage of harmful energy sources like batteries, offering alternatives for wearable and implantable devices where the piezoelectric nanogenerators can be used <sup>8</sup>; an example of this type of system is presented by Lu, B. et al. <sup>9</sup> where a piezoelectric nanogenerator is sutured in the heart of a swine to generate enough electricity to energize a pacemaker and show its viability. As an example of a wearable, Shawon et al. used a film as a nanogenerator that is collocated in a helmet for the monitoring of human movement, showing its capability to perform this action, send signals and recollect energy <sup>10</sup>.

The energy is present in several forms in the environment, from thermal, solar, eolic, nuclear, chemical, mechanical, and more, but between all types of energies, the one that is more common is the mechanical energy because it can be harvested from even tiny biomechanical or mechanical movements <sup>11</sup>, wind blowing <sup>12</sup>, drops falling <sup>13</sup>, vibration <sup>14,15</sup> etc.

The piezoelectric effect is based on the conversion of mechanical energy to electrical energy. There exist two types of piezoelectric effects, the direct piezoelectric effect, and the inverse piezoelectric effect, the direct one is when an external force is applied and it is converted into electrical energy, the inverse one, by the contrary, when an electrical field is applied a mechanical deformation will be caused <sup>8,16,17</sup>.

For an adequate performance of these type of wearable devices, the materials have to comply with some properties as flexibility, biocompatibility, durability, light weight, small size, comfortability, high sensibility and high reliability <sup>4</sup>. Among the piezoelectric materials, a classification can be made of inorganic materials, ceramic materials, polymers, and biomaterials. In the inorganic material class, there can be found materials as ZnO <sup>18</sup>, ZnS <sup>19</sup>, Black phosphorous <sup>20</sup>, Ag <sup>21</sup>, TiO<sub>2</sub> <sup>22</sup>; in the ceramics area the most representative ones are the PZT <sup>23</sup>, BTO <sup>24</sup>, KNN <sup>25</sup>; in the case of the polymers there are the PVDF <sup>26</sup>, Nylon <sup>27</sup>, PLA <sup>28</sup> among others; and with the biopolymers, some natural structures from the body present this type of effect like, collagen <sup>29</sup>, bones <sup>30</sup>, viruses <sup>31</sup>, etc. <sup>4,8,16,32-35</sup>. Inorganic and ceramic materials tend to be brittle and fragile, making it impossible for the nanogenerator to be used as a wearable, despite they have

a better piezoelectric coefficient <sup>33</sup>. Therefore, to provide them more opportunities and advantages, composites between flexible polymers and piezoceramics are done, to get the best part of each of these materials.

For the realization of this thesis project, the chosen polymeric matrix was PVDF. Polyvinylidene fluoride is a semi crystalline polymer that has good flexibility, chemical resistance, thermal and hydrolytic stability, good piezoelectric coefficient, and better mechanical properties than ceramics to be adaptable to the human body <sup>16,36</sup>. It is the most used polymer because of its high piezoelectric coefficient among the polymers. It has a polar crystalline structure that provides the properties to perform the piezoelectric phenomena <sup>37,38</sup>. The molecular structure of this polymer is formed by the monomers (-CH<sub>2</sub>-CF<sub>2</sub>-)<sub>n</sub> <sup>4,38-41</sup>. It has 5 different phases,  $\alpha$ ,  $\beta$ ,  $\gamma$ ,  $\delta$ ,  $\epsilon$ , distinguishing between them the  $\beta$  phase, because in this phase the PVDF presents the highest piezoelectric coefficient by the orientation of its dipoles <sup>8,37,40</sup>. The natural state of PVDF is the non-polar phase  $\alpha$ , but PVDF piezoelectric coefficient can be enhanced by various techniques like addition of nanofillers, mechanical stretching, chemical process, thermal process, and electrical poling, incrementing the  $\beta$  phase percentage <sup>4,42</sup>.

As a technique to enhance the  $\beta$  phase formation the chemical process involves the combination and usage of solvents, the most common is to use polar solvents to enhance the piezoelectric performance of the sensor <sup>42,43</sup>. The selected solvents are DMF because it increases the  $\beta$  phase and it is one of the most utilized solvents for the formation of fibers, also when compared to others it has a great performance <sup>44,45</sup>. It will be mixed with acetone, a volatile solvent, because it has been proved to be a good mixture capable of enhancing the piezoelectric properties of PVDF, the acetone propitiates that the mixed solvents evaporate at a good rate to form the fibers without beads <sup>46</sup>; Ibtahaj, K. et al. evaluated which is the correct ratio of DMF:Acetone showing that it is better to have more acetone than DMF for a proper performance for the Forcespinning method <sup>42</sup>.

Barium titanate (BTO) is a ceramic material with a perovskite type structure that presents a high piezoelectric coefficient with the advantage of being biocompatible and enhancing the performance of the piezoelectric sensor <sup>33,35</sup>.

It has been used as the substitute of PZT (one of the best piezoelectric materials) because this material is not harmful for the environment and health, its low cost and availability in the environment <sup>16,40</sup>. Thus, it is used as a nanofiller in the nanogenerator elaborated in this thesis project.

Graphene is a 2D structure with high specific surface area, good electrical conductivity, superior thermal conductivity, and well mechanical properties, showing its potential to be used for sensors with high mechanical properties, good energy efficiency conversion and high sensitivity <sup>16,24,40,47</sup>. That is why it is used to enhance the conductive properties of the piezoelectric nanogenerator and enhance their performance.

The most common technologies for the fabrication of piezoelectric nanogenerators are spin coating <sup>13</sup>, hot press, electrospinning <sup>11</sup>, solvent casting <sup>48</sup>, and deposition [6, 32]. A new technique called Forcespinning™ with some advantages like the high production rate in a short time, safety for the users, friendly usage, capability to process multiple conductive and non-conductive polymers in front of the most common technique electrospinning was developed by <sup>49-51</sup>. Some piezoelectric nanogenerators are being developed by this technique for example Ibtehaj et al. developed a nanogenerator of PVDF showing that is a promising technique to produce good performance nanogenerators <sup>42</sup>. Therefore, in this project of thesis, the Forcespinning™ is used to elaborate the fibers, showing its capability to produce high performance nanogenerators.

The structure that the piezoelectric nanogenerator could have, is also important, and it can vary from cantilever beam structure, a cymbal structure, stack structure, and the sandwich structure, where the appropriate one for wearable purposes is the sandwich structure due to its flexibility and adaptability to irregular shapes <sup>35</sup>.

In the present thesis project, the working principle of the nanogenerators, applications, methodologies of fabrication, materials, characterizations, and structures will be seen to know the state of the art of these devices. Also, the development and characterization of a piezoelectric nanogenerator has been done from PVDF fibers with BTO and G as fillers and used in combination BTO/G to generate the synergy to increase the piezoelectric properties. Development, analysis of performance and characterization of the device have been done and exposed here.

## **1.1 Motivation**

The fabrication of simple devices that can help make the planet a better place by reducing waste and pollutants and simplify some processes are being investigated. New alternatives are being sought to replace the usage of materials that damage the environment and make a negative impact on this, therefore materials that can produce and harvest energy from sources that were not seen before are becoming more important. Also, materials like these are being used for sensing purposes at the same time they are producing energy like in the body where biomechanical or mechanical energy is produced and not used for anything, creating self-powered sensors that can offer an alternative to equipment that use batteries. This is just one example where this type of device can be of utility but there exist more options for its applicability. It will be shown that the sensor generated in this thesis project, is capable of generating energy from mechanical forces, even when the fiber mat is generated by an alternative technique. By the generation of rich information webs that exchange data through wireless communication protocols, apparatus that can produce data and at the same time power themselves are crucial and will be in the future everywhere.

## **1.2 Problem Statement and Context**

In the near future, the technology will be interconnected, allowing the flow of information in real-time, allowing the monitoring of people or the object to measure, even at long distances, making it possible to reach locations where some services are not present yet. For fulfilling this objective, the creation of devices that generate their own energy without the need of batteries and perform the sensing function, are becoming of great importance.

With the advances in technology in all areas, the methods for acquiring data are also evolving. Smart sensors are the devices that seek to make easier those tasks of obtaining information from a source and sharing it with the users. In the biomedical area, the sensors can go from biosensors, or biomedical sensors that help to monitor different signals from the human body to prevent or treat diseases. Piezoelectric sensors are the choice of this investigation because they can also serve as an electric source for more electronic devices that complete the system to create a smart sensor, or even a sensor by itself, piezoelectric sensors are also called piezoelectric nanogenerators. These sensors can help to detect tiny biomechanical or mechanical forces such a blink of an eye, heartbeat, wind flow, falling droplets and motion of body junctions as other mechanical forces that come from different types of sources.

## **1.3 State of the art**

Several studies have been conducted about the development of piezoelectric devices as this current technology is advancing, so a database search that speaks about the development of these gadgets is presented in the table below and some sensors made using different techniques including the Forcespinning™ technique.



Table 1. State of the art of Piezoelectric nanogenerators and Forcespinning™ sensors

Reference	Objective	Conclusion	Materials	Nps	Solvent	Substrate	Technology	Electrodes	Type
52	Development of a pressure sensor, doping fiber meshes of PVDF with a lanthanide Ce <sup>3+</sup> obtaining a sensor that reacts to the pressure with luminescence	The pressure sensors designed presented an excellent performance offering good results.	1.1 g PVDF CE3+	0.05 g Ce(NO <sub>3</sub> ) <sub>3</sub> ·6H <sub>2</sub> O or Ce(NH <sub>4</sub> ) <sub>4</sub> (SO <sub>4</sub> ) <sub>4</sub> ·2H <sub>2</sub> O	1.95 g Dimethylacetamide 1.95 g Acetone		Forcespinning		Fibers
53	Development of a sensor that changes of color when it detects biogenic amines from food in decomposition, elaborated from conjugated polymers.	Getting promising results for the detection of food that is in bad state	PEG 4 wt% DA 1.6 wt% PDA/TEOS 10:1		sol Ethanol/Choloform 3:1		Forcespinning		Nanofibers
54	Development of nanotubes made from the metal oxides SnO <sub>x</sub> and ZnO to check the sensitivity against hazardous gases.	The results obtained from the tests done, proved the great future that the technology has, to create these sensors by improving the characteristics of the sensors.	PVP 1:1 33 wt% SnO or ZnO 1:1 15 wt%		Ethanol/Dymethylformamide		Forcespinning Solgel		Nanotubes

Reference	Objective	Conclusion	Materials	Nps	Solvent	Substrate	Technology	Electrodes	Type
51	Development of a pressure sensor using the lanthanide $\text{Eu}^{3+}$ using PVDF as the polymeric matrix generating nanofibers with luminescence reacting to pressure. Properties of the sensor are studied.	The sensor showed different behaviors under different pressures exposing a change of luminescence that can be potentially used for other applications as light emitting diodes, bioimaging and scintillators.	PVDF 1.1g $\text{Eu}^{3+}$	$\text{Eu}(\text{NO}_3)_3 \cdot \text{H}_2\text{O}$ 0.5g or $\text{Eu}_2(\text{SO}_4)_3$ 0.5g	1.95 Dimethylacetamide 1.95 Acetone	g	Forcespinning		Nanofibers
26	The creation of a sensor via electrospinning using pvdf is done to experiment and check if the interaction of the developed stacked nanofibers can cause an improvement in the wireless control of human media interface devices.	A successful glove is created that they used to control a toy car wirelessly using and Arduino as the microcontroller. The glove has in each finger a piezoelectric sensor controlling each movement of the car.	PVDF (polyvinile fluoride)				PCB (Printed circuit board)	Direct-Write Near Field Electrospinning	Nanofibers

Reference	Objective	Conclusion	Materials	Nps	Solvent	Substrate	Technology	Electrodes	Type
55	An electrospun sensor was created with PVDF-TrFe nonwoven nanofibers to form a mat to determine an output signal from little movements from the body or cell layers.	The sensors are capable and optimized for small mechanical forces present in cellular mechanics showing a promising future for this sensor with some improvements	PVDF-TrFe 15 % wt HeLa cells		MEK (Methyl Ethyl Ketona)	flexible plastic substrate	Electrospinning	Aluminum conductive tape	Nanofibers
13	The development of a sensor based on BTS-GFF/PVDF by dipping and spin coating is made in this article, capable of measure tiny forces, taking advantage of the changes caused in the material by the low curie temperature.	The sensor can measure tiny forces and even the mimic movement of a balloon showing that it can be used in the healthcare area for many purposes. Even falling droplets	BTS BTO PVDF (coating)		N-dymethylformamide for PVDF	Glass Fiber Fabric	Dipping and Spin Coating	Silver (magneton sputtering)	Thin Films

Reference	Objective	Conclusion	Materials	Nps	Solvent	Substrate	Technology	Electrodes	Type
56	An investigation where the development of a piezoelectric nanosensor was done through electrospinning, they utilized PVDF-TrFe with BZT-BCT ceramic nanoparticles obtaining a sensor with a good performance.	The sensor obtained was able to generate up to 13.01 V and 1.46 $\mu$ W making it able to work as an implantable device or a sensor for motion.	PVDF-TrFe 55/45 proportion solution complete used at 14 wt%	BZT-BCT 40 wt%	Dimethylformide Acetone		Electrospinning	PDMS sheets Au sputtered	Nanofibers
12	A superflexible nanogenerator is developed by the chemical growth of ZnO nanowires in an Al foil covered by PMMA for protection to check if it would work for some applications.	It presented good results, generating an output from wind and from the biomechanical movements of a blink.	ZnO ZnNO <sub>3</sub> .6(H <sub>2</sub> O)0.05M PMMA(coating of ZnO Nw)		HMTA 0.05 M	Al-foil	Chemical growth Spin coating	Al-foil sputtered	Nanowires

Reference	Objective	Conclusion	Materials	Nps	Solvent	Substrate	Technology	Electrodes	Type
18	An ultrathin piezoelectric sensor is created by chemical process on an aluminum foil using ZnO nanowires to investigate the potential of this sensor.	The sensor was collocated in the eyelid of a person getting good results of the movement of the eye underneath. The sensor shows that it could be used for sleeping monitoring and measuring tiny forces.	ZnO PMMA (coating of ZnO Nw)			Al-foil with Anodic Al Oxide	Chemical growth Spin coating	Al-foil	Nanowires
57	In this investigation the authors analyze the changes in the piezoelectric and mechanical properties that the PVDF nanofiber suffer in combination with MWCNT	They concluded that with the addition of MWCNT the nanofibers enhance both the piezoelectric and mechanical.	PVDF	MWCNTs 0.008 wt%	Dimethylsulfoxide (DMSO) Dimethyl Ketone		Electrospinning	Aluminium Taping with indium tin oxide coated PET	Nanofibers

Reference	Objective	Conclusion	Materials	Nps	Solvent	Substrate	Technology	Electrodes	Type
22	The elaboration of a piezoelectric film is done with the use of TiO <sub>2</sub> coated with dopamine particles to enhance the piezoelectric, phase formation of PVDF. Dopamine improves the compatibility between components	The enhance of the properties is achieved with the use of dopamine the compatibility of the matrix with the particles is better. Can be used for portable and wearable devices,	PVDF	TiO <sub>2</sub> alone 5wt % TiO <sub>2</sub> 5wt%coated with dopamine 2.0g	Dymethylformamide	ITO	Solution casting methods Solvothermal	Gold	Films
48	The fabrication of a flexible thin film nanogenerator is produced by the authors made of MoS <sub>2</sub> -rGo-PVDF to study the piezoelectricity property	A nanogenerator is successfully created, proposing a mechanism for enhancing the piezoelectricity of the nanogenerator.	PVDF 1g	MoS <sub>2</sub> -rGo 100mg	Dymethylformamide 10 ml		Solution casting	Al/Au	Films

Reference	Objective	Conclusion	Materials	Nps	Solvent	Substrate	Technology	Electrodes	Type
14	The fabrication of a piezoelectric sensor made of PVDF-HFP with carbon quantum dots to improve its performance by the characteristics of the added nanoparticles. Some applications for the flexible piezoelectric sensor are explored.	The performance of the sensor with the carbon quantum dots improved in comparison with the film of PVDF-HFP alone. It shows great sensitivity, and it was proposed for some applications like voice recognitions, finger bending detection, and vibration monitoring.	PVDF-HFP 1.5g 3:2 w/so	CQDs 2mg	Acetone/Dimethyl formamide 20ml	PEN-ITO	Spin-coating	PEN-ITO	Films
42	The development of a nanogenerator self-poled through a novel centrifugal technology is done to study if the nanogenerator would have a good performance. The nanogenerator is made of PVDF.	The nanogenerator proposed is achieved having a great performance generating 22 V <sub>oc</sub> using a simpler, affordable, and safer technique. It shows great potential for several applications in harvesting energy and as sensors by its long life, mechanical durability and good piezoelectric performance	PVDF 0.12g/mL		Acetone/Dimethyl formamide 7:3 8000 rpm		Forcespinning	Nickel based fabric tapes	Fibers

Reference	Objective	Conclusion	Materials	Nps	Solvent	Substrate	Technology	Electrodes	Type
11	Development of a sensor based in PVDF nanofibers with a 3D structure coating. The coating was made of ZnO nano rods for enhancing the output and sensitivity of the sensor, to detect different signals for monitoring people's health	The development of the sensor is achieved showing that it is durable and sensitive for detection of signals like respiration, pulse rate and muscle motion	PVDF 25 wt%	ZnO nanorods	Acetone/Dimethylacetamide 5:5 v/v	PU tape	Electrospinning	Ag Nano wires	Fibers



## **1.4 Objectives (General Purpose)**

To develop a piezoelectric smart device with nanofibers meshes elaborated by Forcespinning™ technique using complementary fillers BTO, G, and BTO/G for the enhancement of the piezoelectric properties of the polymeric base material PVDF, with the capability to generate energy from mechanical forces.

### **1.4.1 Specific Objectives**

- Synthesis of BTO nanoparticles by the solgel method for their usage as a filler dopant in the fiber meshes
- Fabrication of fiber meshes of PVDF with G or BTO fillers by Forcespinning™ technique.
- Fabrication of the synergy meshes of PVDF with G and BTO fillers by Forcespinning™ technique.
- Development of a piezoelectric nanogenerator device based on nanofibers of polyvinylidene fluoride.
- Chemical and physical characterizations of nanomaterials fillers, fiber meshes and piezoelectric device.

## **1.5 Hypothesis**

The fabricated device of PVDF through Forcespinning™ technique will be flexible, and light to adapt to the structure of the body or any area. Its sandwich structure design will help to give the device a long lifetime of use. It is going to be simple by the process of fabrication. The sensor will be able to produce signals from mechanical movements.

## 1.6 Scope

The scope of this thesis project is the development of a piezoelectric smart device based on fiber meshes of PVDF as the polymeric matrix with the addition of fillers as BTO, G and BTO/G for the enhancement of piezoelectric properties through the Forcespinning™ technique. To assess its capability to generate energy by mechanical forces.

## 1.7 Dissertation

**Chapter 1** offers an introduction to the topic to let the reader know about what we will treat in this thesis project, and a brief overview of the state of the art is covered by analyzing the piezoelectric devices that were done through Forcespinning™ and piezoelectric sensors that fall into the area of wearable gear.

**Chapter 2** presents an overview of the theoretical aspects from the piezoelectric phenomena, internet of things, smart sensors, manufacturing techniques, piezoelectric materials, and the characterization techniques for the piezoelectric devices are described.

**Chapter 3** shows the methodology that was followed for the construction of the piezoelectric device, since the synthesis of the filler materials to the design and elaboration of the piezoelectric sensor. Characterization was performed following the conditions and procedures of the machines presented in this chapter.

**Chapter 4** presents the results obtained from the characterization techniques and are discussed.

**Chapter 5** presents the conclusions reached and highlights the contributions.

**Chapter 6** shows future research work.

## 1.8 Solution Overview

A piezoelectric device based on PVDF with the addition of BTO and G will be performed through the Forcespinning™ technology to elaborate fibers that will be sandwiched between copper tape films that will serve as the electrodes, and as an external protective layer and substrate polyamide tape will be collocated in each electrode, together forming the apparatus that could be able to produce energy from mechanical forces.

The development of the smart device will be done with the fabrication of fiber meshes through the Forcespinning™ technique. The fibers are going to be observed to know their morphology and composition then it will be placed between thin metal foils that will work as electrodes. The electrodes will be connected with copper wires and then a coating of polyamide will be placed all over the sensor for protection. The mechanical properties of the whole sensor integrated will be studied. The copper wires will be connected to an electrometer and an oscilloscope to observe and measure the electrical signals.

## Chapter 2

### 2. Theoretical Aspects

#### 2.1 Internet of Things

In the actual time, more apparatus are being connected to the internet forming, a system that can work with all the devices interconnected between them, allowing the exchange of information and control of several operations <sup>5</sup>. These technological advancements enhance the creation of new systems capable of simplifying tasks. To achieve the interconnection of the electronical equipment connected to the internet, the IoT system needs an architecture to accomplish this task, the architecture that will be explained is the five-layer architecture, where the layers are business layer, application layer, service management, object abstraction and object layer <sup>2,5</sup>. Those layers will be described in table 1:

Table 2. IoT five-layer Architecture.

Layer	Definition
Object Layer	Sensors and actuators that recover data and perform some actions
Object Abstraction Layer	This layer communicates the data through communication protocols to the service management layer.
Service Management Layer	In this layer the service and user are paired to deliver the correct service, and make choices
Application Layer	In this layer, the user can observe the data that he asked for an interface or his device
Business Layer	This layer manages the full services that the user is requesting with the use of workflows, it also monitors and evaluates the service to enhance it

The layer where the smart sensors belong is the object layer, cause in this one, all the objects that recover data from the real world as sensors and actuators are involved. The aim of the IoT is to create smart systems that can interact between them creating a better controllable process where it is implemented, for example, smart cities. To communicate between the devices, there must be some communication protocols to obtain good channels for the exchange of information; some of these protocols based on the web service are XML/HTML, EXI, TCP/HTTP, CoAP/UDP, IPv6/IPv4, WPAN <sup>3</sup>.

With the help of this IoT environment the creation and development of new smart wireless sensors is possible because it will be constructed in a communication rich ambient to deliver data and act depending on the results of that data.

## **2.2 Smart Sensors**

For a better perception of what a smart sensor is, a definition for a sensor will be explained, a sensor is a device that retrieves signals from an external factor that wants to be controlled or monitored and then that signal is converted to an electrical signal to be processed and used <sup>58</sup>. Smart sensors according to the IEEE in the specification 1451.2 says that a smart sensor is a device that performs functions beyond its normal functionalities, integrating the transducer in the sensor for a networked environment <sup>59</sup>.

The basic functions that a smart sensor must have, are the sensing element, power management, communication storage, data processing, calibration, and signal conditioning <sup>58</sup>. Therefore, for the construction of a smart sensor the components that this type of equipment must have, are, a microcontroller, a communication module, the sensor device, and an electrical circuit to manage the signals and with all these components, build a system for collecting the electrical signals, communication, and processing. The sensing component will be in charge of getting the electrical signals that want to be measured, using the integrated communication module to send them to the microcontroller to be processed and used for a purpose. In the area of the internet of things, the smart sensor requires some crucial functionalities by the demand of the applications, the functionalities are ultra-low power consumption, low cost, ultra-small size, low maintenance, practical and high performance <sup>58</sup>.

Self-powered sensors are devices that generate their own energy to power all the circuits that are connected to the sensor to perform their tasks, allowing their implementation without batteries, making more efficiently their duties, the energy is gathered from the external natural energy that is present in the ambient, *random energy*

<sup>60</sup>.

Sensors are driven by several factors that affect them and have to be considered when the sensor wants to be applied. Some characteristics that the sensors present are linearity, hysteresis, response time, sensitivity, and signal to noise ratio <sup>61,62</sup>.

In the healthcare area, several types of sensors are used for multiple applications, but we will focus on the area of the wearables. In this area, sensors could be classified for their operating mechanisms for collecting information, here are some of them, resistive, capacitive, piezoelectric, piezoresistive, piezothermic, triboelectric, bioelectrical impedance, electrochemical and optical and all these smart sensors are used for the detection, monitoring, and treatment of diseases <sup>7</sup>.

### 2.3 Communication Protocols

In order to communicate between devices, the wearable sensors need some communication protocols to achieve the exchange and representation of information. A network area for the communication of these sensors has been developed, called personal area network (PAN) or body area networks (BAN), with their proper architecture for the communication protocols, starting with the Intra-BAN, Inter-BAN, and Beyond-BAN that will be explained in the table below <sup>63</sup>.

Table 3. Communication Architecture for Wearable Devices.

<b>Classes</b>	<b>Definition</b>
Intra-BAN	Communication between the sensors and personal servers.
Inter-BAN	Communication between servers and more access points like cellphones, computers, etc.
Beyond-BAN	Communication in a metropolitan area accessing to the information via internet

In the Intra-BAN layer, the technologies and standards that are used for the communication of data are Bluetooth LE, NFC, Zarlink, Zigbee, Sensium, RuBee, ANT, and BodyLAN.

Bluetooth low energy (BLE) is a good choice for the implementation as the communication protocol, because it is a protocol that uses low power, saving energy and making more efficiently the work, it also works in frequencies that do not affect the user's health, highlighting it as a good option for wearable sensors <sup>64</sup>.

## 2.4 Piezoelectricity

The piezoelectric word comes from the Greek word *piezein*, that means pressure, and electricity, therefore the generation of electricity by pressure <sup>16,65,66</sup> and it was first used by Hankel in 1881 <sup>8</sup>. The piezoelectric phenomena was found by Curie brothers in 1880, while they observed that an electric charge was generated when a force was applied to a quartz crystal and a deformation in the material when it was exposed to an electric field <sup>17,35,65,67</sup>. Within this piezoelectric phenomena, two effects can be observed, the direct piezoelectric effect that deals with the conversion of mechanical forces that are applied in the piezoelectric material into electrical charges; and the inverse piezoelectric effect that deals with the physical deformation of the piezoelectric material when an electric field is applied to it <sup>8,16,17,32,66</sup>. This effect happens because in the crystal structure of these piezoelectric materials there are present positive and negative charges that neutralize between themselves when it is in a relax state until an external force is applied separating the positive and negative charges to each surface generating a dipole, therefore generating electrical energy from this deformation <sup>8,17,32,66</sup>. Refer to figure 1 to observe the phenomena graphically. Some materials that present this type of effect are single crystals, ceramics, polymers, composites, and relaxor-type ferroelectric materials <sup>17,68</sup>. The direct piezoelectric effect materials are most used as sensors that can detect movements, acceleration, pressures, forces, vibration changing the mechanical signals into electrical signals to be analyzed <sup>32,35,65</sup>. And materials with the inverse piezoelectric effect are used as actuators by the deformation that is caused in them by an applied electrical signal <sup>35</sup>. The piezoelectric energy generation is a promising alternative for a cleaner way of obtaining electricity due to the advantage that the mechanical energy that is present in all the activities and in our environment. It also presents a higher energy density than other mechanisms as electrostatic and

electromagnetic making it the best option for the use in several applications and areas 35,68 .

The constitutive equations that are used for the description of the piezoelectric phenomena are:

(Eq.1)

$$D = dT + \epsilon E \text{ (Direct effect)}$$

(Eq.2)

$$X = sT + dE \text{ (Converse effect)}$$

Where the D, is the electric displacement, d is the piezoelectric coefficient of the material, T is the stress exerted,  $\epsilon$  for the permittivity of the material, E for the electric field, X strain, and s for mechanical compliance <sup>35</sup>.

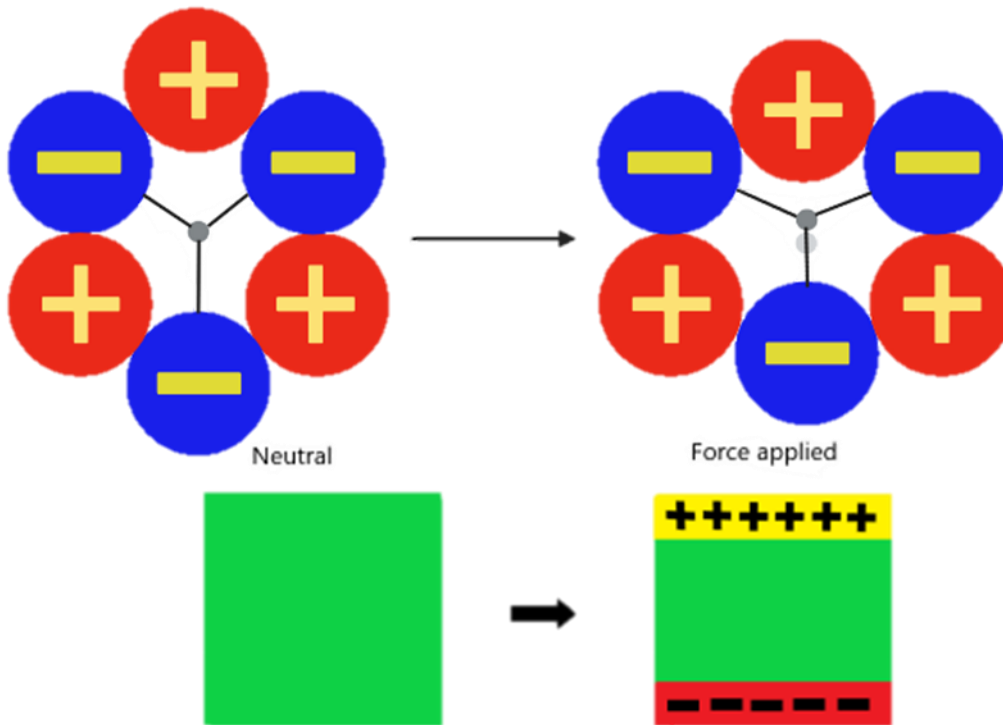


Figure 1. Piezoelectric phenomena



## 2.5 Device Structures

For the use of these types of piezoelectric nanogenerators, some structures have been applied to the materials to increase the performance of the device. The most typical structure that is utilized and most studied is the cantilever beam structure. It is based on the utilization of the piezoelectric material between the electrodes like in a sandwich structure, with a mass tip at the end of one side of the component to adjust to the frequency of the system where it is collocated. This type of structure cannot retrieve enough energy from the body by the frequency and amplitude of vibrations. Also, its clearly fragile and bad adaptability to the shapes of the body <sup>15,34,35</sup>. Another structure that is used for piezoelectric nanogenerators is the cymbal structure and it is based on a piezoelectric disk, collocated between two metal cymbal endcaps. It works well for high loads, increasing the resistance and life of the piezoelectric material <sup>34,35</sup>. The other structure is called stack structure and is based on the gathering of several piezoelectric layers to improve the voltage output <sup>34,35</sup>. Last, is the sandwich structure that is an easier structure to build and with high mechanical stability, it will also help to increase the lifetime of the device and adaptability to irregular shapes. It is based on the sandwiching of a piezoelectric material between two electrodes <sup>15,35</sup>. Therefore, this structure is the one selected for the properties that we could have in our sensor for wearable purposes like flexibility and adaptability.

## 2.6 Mode of Operation

There exist two operation modes that are named by the direction in which the force is applied to the piezoelectric material and the polar axis of the material. The nomenclature works in this way, the first number represent the direction in which the materials is polarized, or how the flow of electrons will be, and the second number of the coefficient represent the direction in which the force is applied. For the piezoelectric materials the first number is “3” for the polar axis. In the case of the force applied the “3” represents the force in the same direction as the polar axis and the “1” represents the force along the thickness of the device, perpendicular to the polar axis <sup>17,34,35</sup>. Creating the operation modes  $d_{33}$  and  $d_{31}$ , with the first one describing that the force applied is parallel to the polarization axis and the second one with the force perpendicular to the polarization axis. Other type of mode of operation exist that describes the shear piezoelectric coefficient  $d_{15}$  where the polarization axis is inclined to the applied force <sup>69</sup>.

## 2.7 Piezoelectric Materials

The materials which present that effect of producing an electrical charge when a force is applied, all of them is thanks to the crystal structure that they have, with no symmetry center <sup>17,67</sup>. The variety of materials that have this type of effect go from, single crystals, ceramics, polymers, biopolymers, and ferroelectric <sup>17,32,68</sup>. The first material that was discovered having this effect by the Curie brothers was the quartz crystal, even it has a low piezoelectric coefficient. The most relevant first application that the quartz had, was during the first World War for the improvement of the performance of a sonar detector and later while the World War 2 was happening the ferroelectric materials were found with better piezoelectric coefficients than the crystals used before <sup>67</sup>. Ceramics began to be utilized by most of the researchers, they found that the relaxor lead titanate crystals and lead based ceramics had better piezoelectric properties than the other piezoelectric materials, but due its toxic nature to human health and environment the area of research has moved to lead-free materials that can replace the use of lead materials in devices <sup>33–35,67</sup>.

Barium titanate is one of the ceramic materials that can help to replace the lead materials, because it has a high piezoelectric coefficient in comparison with the other piezoelectric materials, low cost, not harmful for the environment and is present in great quantities in nature <sup>16</sup>. Ceramics are materials that are brittle and fragile, so for applications where flexibility is needed those materials are not the adequate one, therefore a way to address this problem is the formation of composites. Piezoelectric polymers represent the opportunity, in combination with ceramic, ferroelectric or/and conductive fillers, to create smart materials with high piezoelectric coefficients and flexibility for applications that requires it <sup>8,34</sup>. PVDF is a piezoelectric polymer which piezoelectric effect was found in 1969 by Kawai and possess the highest piezoelectric coefficient among the piezoelectric polymers <sup>16,34,35</sup>. Therefore, this material is used as a polymeric matrix for the development of flexible sensors that resist the irregular shapes of the body in cases of wearable devices and the forces at which they are exposed. But this is only one of the polymers that are used, other polymers are such as polylactic acid, nylon, polyurea, silicon and epoxy <sup>33</sup>. Other way in which investigators address the problem of the flexibility in the ceramic ferroelectric materials is by the creation of materials with stretchable structures when they are developed as thin films, that allow these materials to be used in applications where flexibility is needed, some of these mentioned structures are kirigami layouts, serpentine layouts, fractal patterns, helical structures and woven <sup>8</sup>.

Biomaterials are not out of the scope, because also some of them present piezoelectric characteristics that can be used for the creation of devices, like collagen, peptides, viruses, DNA and more <sup>4,16,32</sup>.

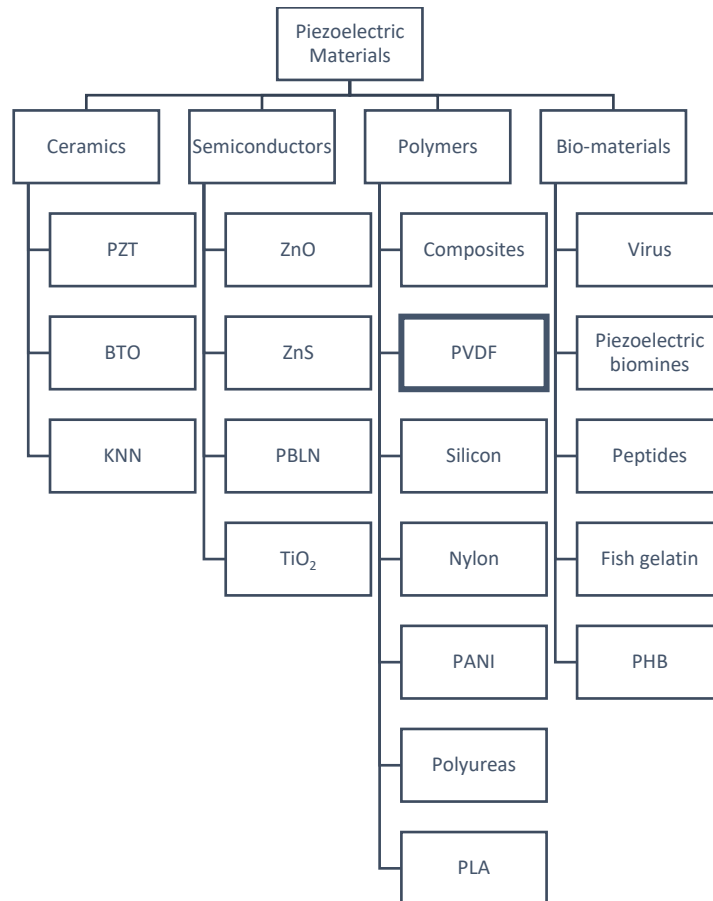


Figure 2. Piezoelectric Materials

## 2.8 PVDF

PVDF is a thermoplastic polymer with a semi-crystalline structure that can be present in five phases  $\alpha$ ,  $\beta$ ,  $\gamma$ ,  $\delta$ , and  $\epsilon$ , highlighting between them the  $\beta$  phase, because this is the phase that presents the best piezoelectric phenomena unlike the other phases. This is due to the molecular structure that this phase presents where the atoms of the molecules forms dipoles well separated at each side of the structure<sup>50</sup>. The  $\beta$  phase is the most piezoelectric due to the all-trans (TTTT) conformation that it presents, presenting the best behavior for pyro-, ferro- and piezoelectric phenomenas<sup>70,71</sup>. Some of the principal characteristics that this polymer and its copolymers present are that they possess a great chemical resistance, high mechanical strength, abrasion resistance, low permeability to most gases and liquids, nuclear radiation resistance, processable, thermal stability, hydrophobicity, electrochemical resistance, and uv-resistance<sup>16,41</sup>.

The molecular structure of this polymer is formed by the monomers  $(-\text{CH}_2-\text{CF}_2-\text{n})$ <sup>4,38-41</sup>. The molecular weight of the polymer plays an important role at the hour of forming the fibers because it is demonstrated that with a higher molecular weight the  $\beta$  phase was enhanced by the higher viscosity of the solution<sup>72</sup>.

The natural state of PVDF is the non-polar  $\alpha$  phase, but PVDF piezoelectric coefficient can be enhanced by various techniques like addition of nanofillers, mechanical stretching, chemical process, thermal process, and electrical poling, incrementing the  $\beta$  phase percentage<sup>4,42</sup>.

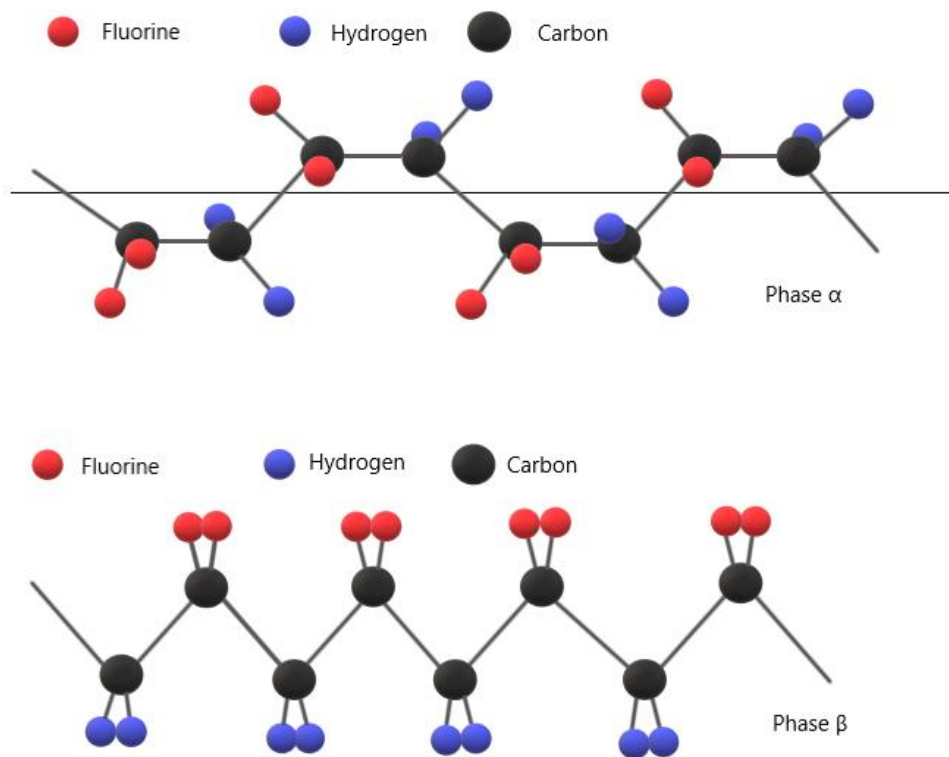


Figure 3. PVDF molecular structure for  $\alpha$  phase and  $\beta$  phase

## 2.9 Nanofillers

Thus, by the characteristics of the polymeric materials, the lower piezoelectric coefficient that limits their use, is addressed in the form of the addition of fillers. Most of the ceramic ferroelectric, and semiconductors materials are used as nanofillers for this

purpose, where we can find materials as PZT, BT, KNN, ZnO, TiO<sub>2</sub>, Bi, ZnS and black phosphorous<sup>8,32,33,35</sup>.

Apart from piezoelectric nanofillers other type of fillers are used for the enhancement of the performance of the nanogenerator, conductive nanofillers are used in the creation of composites to help the transfer of energy and promote the formation of the β phase of the PVDF, which is the desired one by its high piezoelectric properties. The conductive nanofillers that are used are graphene, carbon nanotubes, carbon black and silver among others<sup>35</sup>.

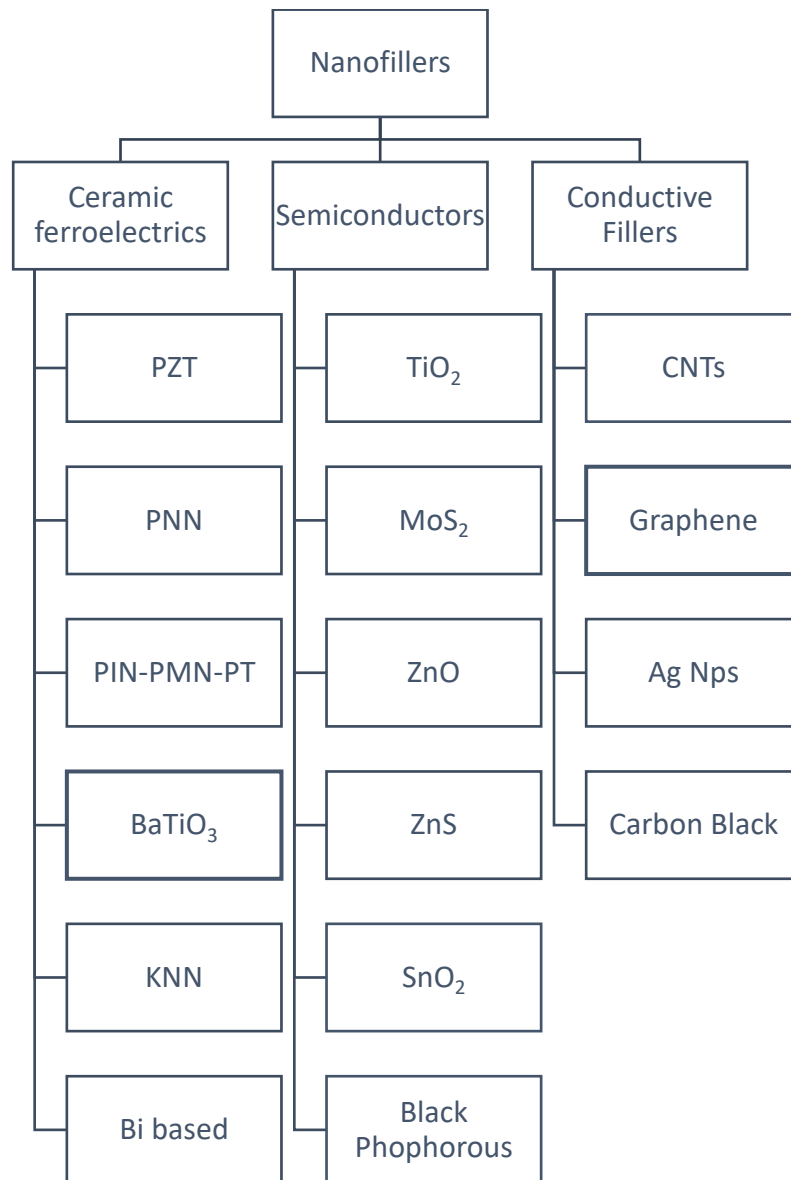


Figure 4. Piezoelectric nanofillers

## 2.10 Solvents

For the selection of the solvents the ones that are utilized to propitiate the formation of the  $\beta$  phase, are the high polar solvents, like dimethylformamide (DMF), dimethyl sulfoxide (DMSO), dimethylacetamide (DMA), tetrahydrofuran (TFH), N-Methyl-2-pyrrolidone (NMP), Trimethyl phosphate (TMP), Triethyl phosphate (TEP), Hexamethyl phosphor amide (HMPA) and, Methyl ethyl ketone (MEK). Between all these solvents where the PVDF has been dissolved, the ones with the best results are DMF, DMA, DMSO and HMPA, highly polar solvents that are capable to promote the change of  $\alpha$  phase to  $\beta$  phase <sup>43–46,73</sup>. There are several some contradictions between the articles because in some the DMSO has a better performance than the DMF and in other article the DMF is mentioned as a better solvent in comparation with it. It is true that there is a desire to change from DMF to DMSO because the DMF is considered as a hazardous and toxic solvent, and DMSO is not <sup>45</sup>. Also, the usage of only the polar solvent is counterproductive because of the high boiling temperature that the DMF has, causing that the fibers are not well formed by the content of solvent they have even after the nanofiber formation. Therefore, mixture of solvents is used to promote a higher evaporation rate just enough to allow the formation of nanofibers with high content of  $\beta$  phase, acetone is a volatile solvent that can be used for this purpose <sup>37</sup>. In the case of the Forcespinning™, it was found that the concentration of the acetone has to be higher than the concentration of DMF to promote PVDF solidification <sup>42</sup>.

## 2.11 Substrates

For the wearable applications flexible materials that can offer more durability and protection to the electrodes and the piezoelectric nanogenerator are preferred. Flexible insulating polymers are used to fulfill this objective, some commercial materials as PET/ITO thin films, Kapton (polyimide tape), silicon films are some of the ones selected by researchers to develop their projects of piezoelectric nanogenerators creation, or thin films of polymeric materials that are produced using different techniques like spin coating, dip coating, electrospinning, etc. The flexible substrates have to comply with some properties that are needed to have for electronic applications as flexibility,

transparency, stretchability, lightness, insulation and strength <sup>32</sup>. Not only the substrate is sought to be flexible, also there exist an intention of creating flexible electrodes for the applications of the electronic devices that are going to be made using the piezoelectric nanogenerators and do not affect the performance of this by using not adequate materials. Some materials that comply with these properties are conductive polymers, soft ionic hydrogels, liquid metals, elastomer with conductive fillers (CNT, metal NWs and NPs) <sup>8</sup>.

## 2.12 Fabrication Techniques

The elaboration of this piezoelectric devices has been done through multiple techniques by which the characteristics and the shape of the final product are changed and manipulated through all these techniques. Within them we can find techniques like electrospinning, additive manufacturing, spin coating, deposition, hot press and Forcespinning™ are some of the techniques utilized for this purpose. Electrospinning being the favorite for the creation of nanofibers <sup>8,16,32</sup>. A diagram showing the most common techniques for the fabrication of piezoelectric sensors is showed below.

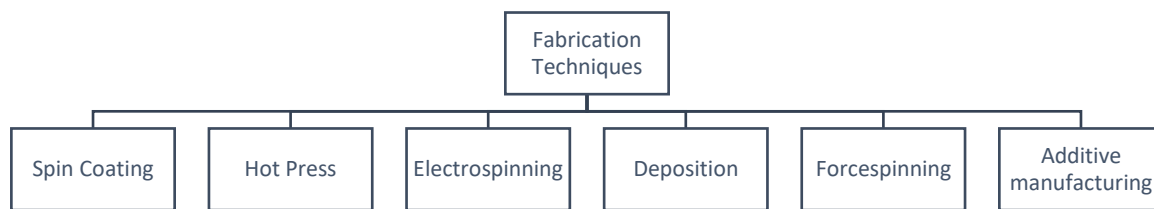


Figure 5. Fabrication Techniques for Piezoelectric sensors



### **2.12.1 Electrospinning**

Mentioned as the most promising technique for the elaboration of nanofibers, is based on the extrusion of liquid polymer with the help of a syringe pump, pushing the solution through a needle, which is exposed to an electric field causing that the electrostatic forces break the surface tension of the solution forming nanofibers while the solvent evaporates until it reaches the grounded collector <sup>37,38,44</sup>. It is the most used technique for the creation of nanofibers <sup>8</sup>.

### **2.12.2 Additive manufacturing**

With the advances in the technology and materials, some piezoelectric materials are generated and adapted for their usage in 3D printing, where customizable and specific devices can be done with a high accuracy for its application. It is based fundamentally on the creation of piezoelectric equipment layer by layer using the materials with the wanted properties in the desired shape with a great accuracy <sup>16,32</sup>.

### **2.12.3 Spin Coating**

The spin coating technique is based on the usage of centrifugal forces to spread a drop of a solution over a smooth plate that rotates at high speeds generating thin films of the desired material. The properties that can be managed from this technique for the enhancement of the films are rotation time, speed, and quantity of solution <sup>36</sup>.

### **2.12.4 Deposition**

Some piezoelectric materials are also deposited over substrates to create nanowires or thin films of the materials to create piezoelectric devices. It is based on the deposition of materials layer by layer using the atoms of the materials. It is developed inside a chamber and there exist several methods to deposit materials. Physical vapor deposition and chemical vapor deposition are the main techniques from where all the others are derived <sup>61</sup>.

### **2.12.5 Hot Press**

The hot press technique is based on pouring a solution over a substrate, where it can be also used, solutions with piezoelectric materials, for then to be pressed and heated, near its melting point, until the final piece is obtained. It can be used for the obtention of pieces with a specific shape. The pression and temperature applied enhance the compaction of the crystal structure of the material improving its piezoelectric behavior <sup>36</sup>

### **2.12.6 Forcespinning™**

This is a technology that uses centrifugal forces to create fibers of a wide variety of polymeric materials, conductive and nonconductive. While the polymer solution that is inside the spinneret, the part that contains the solutions and turns around for the extrusion of the fibers, the solution that goes out begins to elongate, evaporating at the same time the solvents, forming the fibers until they reached the collector. It was developed to substitute the electrospinning technique. It offers the mass production of fibers, environmentally friendly and with a great variety of materials for their printing because this technology does not limit only to materials with electric conductivity. It is a safer technique because it does not involve high voltage that can be dangerous for the health of the people <sup>49,54</sup>. This technique also presents the alternative to work as a melt spinning technique where the polymer is melted in the same machine and left to fall inside the spinneret, to then fabricate the fibers <sup>74</sup>. The factors that affect the Forcespinning™ process are the angular velocity of the spinneret, the cycle time, the distance from the collector to the out of the spinneret, viscosity of the solution and the diameter of the orifice of the spinneret <sup>74,75</sup>. Also, other external factors like humidity affect the process of fiber formation by the high degree of humidity in air, making more difficult the solvent evaporation, temperature is another factor that plays a role in the same process of solvent evaporation. See Figure 5 for the internal diagram of the Forcespinning™ technique.

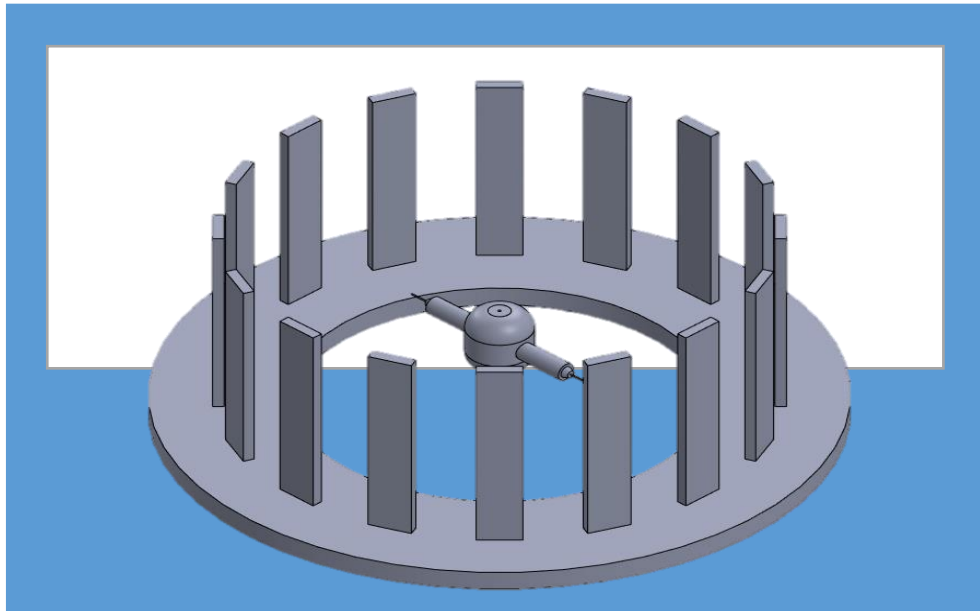


Figure 6. Forcespinning™ technique diagram

### 2.13 Structures of Materials

The nanostructured materials can be classified by its dimensionality (0D, 1D, 2D and 3D). The scale range to consider that a material is nanoscale is below 100 nm.

Nanofibers are 1D nanomaterials that has two of their dimensions in the nanostructure scale, they have a great specific surface area.

Thin films are 2D nanomaterials when they are ultrathin films, and they have only one dimension in the nanoscale range, they have good specific surface area compared with the bulk material <sup>76-78</sup>.

Nanofibers are a better option than the films because they present a better performance than the films by the larger specific surface area, higher damage resistance and flexibility <sup>79</sup>.

The alignment of the fibers plays an important role cause the alignment can influence other properties that are in our device. The mechanical properties are influenced by the

orientation of the fibers, cause thanks to that alignment the forces that are applied into them, can be evenly distributed between the fibers increasing the tensile loads that they can bear. The tenacity and the initial modulus of the fibers are enhanced by this alignment of the fibers, while with the random fibers these values are the lowest. Also, the elasticity of the fibers is increased <sup>57</sup>. According to Mamidi et al., where a study was realized about the Forcespinning™ technique, the alignment of the fibers can be achieved at lower running times <sup>80</sup>. The morphology of the fibers also impacts the performance of the device, some structures that can be present in the fibers are studied, the structures are, wrinkled, smooth and porous, where the one with the best performance for the generation of electrical charges is the wrinkled one because of the friction that can be caused between the aligned fibers <sup>81</sup>.

Other options for the structure of the materials that are utilized for the construction of piezoelectric devices with good performance are nanowires NW, nanoparticles NPs, nanotubes, and nanorods <sup>82</sup>.

## **2.14 Applications**

Piezoelectric nanogenerators are used in several areas, depending on the application the materials and structure of the sensors can change because of the different conditions at what the devices may be exposed while they are working.

### **2.12.1 Healthcare**

In the healthcare area piezoelectric nanogenerators are used for the monitoring, prevention, and treatment of diseases <sup>7</sup>. They are also used as an alternative for batteries because they can be used to energize other circuits that are connected to them, supplying energy for them to function, in the case of implantable devices <sup>83</sup>. The sensors for this area are divided between implantable, and wearable, the implantable goes inside the body, of course using biocompatible materials that does not affect the

health of the user, and the wearables goes in the external part of the user as an accessory <sup>84</sup>. Yang et al. created a sensor that is utilized for the monitoring of the respiration frequency, they can differ between when the person is grasping, breathing normally and a deep breathing, they can also retrieve signals from wrist pulse and muscles, they developed a piezoelectric sensor by growing ZnO nanorods in electrospun nanofibers <sup>11</sup>. Mahanty et al. developed an electronical skin (e-skin) utilizing a piezoelectric sensor based in electrospun nanofibers with MWCNTs for the monitoring of the movements of patients in hospitals <sup>85</sup>. In most of the cases in this area the piezoelectric sensors have a sandwich structure.

### **2.12.2 Buildings and Infrastructure**

In the construction area these type of devices are used as sensors for the monitoring of the structural health of the buildings, to prevent accidents and give the proper maintenance to it. Also, as energy generation the piezoelectric materials are used in combination with the materials for the construction, like in buildings, bridges, asphalts, floor tiles or sidewalks to recover energy from the usual activities that happen in them, like the transiting cars, and walking people, the energy gathered could be used to power principally luminaria, signals and even the business where they are placed <sup>68,86-88</sup>. The study of the power generation by the high traffic in highways is studied by the design of a piezoelectric sensor that could be placed in a road under the pavement <sup>89</sup>. Also, a study was realized where it is show that is feasible to use the electricity generated by footsteps utilizing piezoelectric sensors to provide electricity to places where the traffic of people is high like malls, bus terminals and shopping centers<sup>90</sup>.

### **2.12.3 Vehicles**

With the coming of electrical vehicles to change from generating power from oil fuels that are highly pollutant to self-sustainable energy and IoT systems creating smart vehicles, new ways for monitoring and generating electricity are needed to support these applications inside the vehicles <sup>91</sup>. Some studies are developed to study how the piezoelectric nanogenerator can help to harness the mechanical energy that is waste and convert it into electrical energy, Mouapi et al. showed that is possible to create a device that can convert the vibrations generated by a car and transform them into electrical energy to power WSN (wireless sensor networks) <sup>92</sup>. Also, in oceanic vehicles the search for the harnessing of the mechanical energy generated by the mechanical components of the vehicle to transform it into electrical energy takes place, and it is proven that it could be a good system to produce electrical energy, Li et al., developed a piezoelectric device that is used to produce this type of energy from the suspension of the oceanic vehicle<sup>93</sup>. Other types of applications that are present in the vehicles is the monitoring of the health structure of aerospace vehicles and the health structure of rails, to check the integrity of the parts and give the proper maintenance to them <sup>84,94</sup>.

### **2.12.4 Industry**

At the industry several machines and equipment have the requirement of be constantly supplied with energy, and a lot of the mechanical energy produced in there, like vibrations of machines is wasted, therefore, to take advantage of this energy piezoelectric materials can be used to gather all this energy and focus it on applications that need it, also the vibrations caused by the environmental energy can be of use for this purpose <sup>36</sup>. Also, these materials can offer a new way of monitoring the health of their machines and equipment that require it, for example Khazae et al. 2019 uses an apparatus based in a piezoelectric sensor that is designed for the remote monitoring of rotating machines using these self-powered devices avoiding the need of wires and saving money by not doing this wiring, and Nguyen et al. 2022 realized the conditioning monitoring of a critical part of some machines, the bearing, that is monitored through a

3D printed piezoelectric sensor <sup>95,96</sup>. Soft robotics is a new area where these sensors can be functional, the development of a piezoelectric sensor for gesture recognition is done to control a robotic hand showing the big potential that this technology has, the device is formed by electrospun nanofibers of PVDF with ZnO particles with cowpea structure <sup>97</sup>.

## Chapter 3

### 3. Materials and Methods

For the development of a piezoelectric device, fibers were realized using PVDF as the polymeric matrix with BTO and G as nanofiller dopants. The following experimental strategy was carried out and will be described.

#### 3.1 Materials

PVDF materials was obtained from (Sigma-Aldrich Toluca), it has a molecular weight of 534,000 and comes in the form of powder. G nanopowder was obtained from (Nanostructured & Amorphous Materials, Inc) and they have a diameter size of 2 – 10 um from 2 to 3 layers. Barium Acetate was obtained from (“Baker Analyzed” REAGENT) and Titanium Butoxide was obtained from (Sigma-Aldrich) to perform the sol-gel synthesis process of BaTiO<sub>3</sub>. Acetone and Dimethylformamide were obtained from (DEQ) and (Sigma-Aldrich) respectively. Copper foil tape was obtained from ELK and the Polyimide tape from (Advanced Polymer Tape).

#### 3.2 Methodology for preparation of Barium Titanate

For the obtention of Barium Titanate (BaTiO<sub>3</sub>) see Figure 6; Barium acetate was mixed in a solution with acetic acid, H<sub>2</sub>O and ethanol in a flask with a reflux column to avoid solvent evaporation. Then it was stirred for 4 hours. Next, the Titanium Butoxide was mixed with the solution in constant stirring, drop by drop and left in constant stirring around 60°C and 500 rpm for 1 day. After this, more water was added to the mix and stirred during 3 hours for gelation. Then the solution made was collocated in an oven for drying at a temp around 90°C for 1 day. The materials obtained after the drying process were grinded by hand in a mortar until a fine, same color powder is obtained. The powder was put on a melting pot to calcinate it around 900 °C for 3 hours and left it to cool inside the furnace.



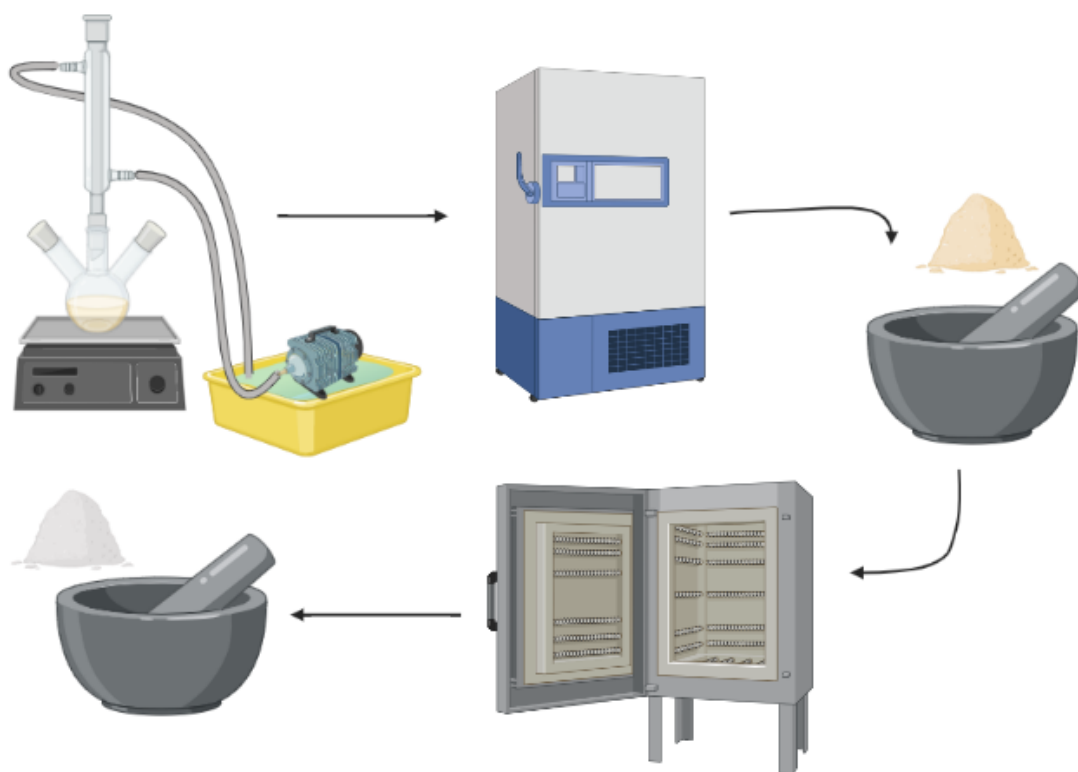


Figure 7. Diagram of synthesis of BTO.

### 3.3 Solution preparation

The parameters that were visually found to be the best for the formation of fibers were 5000 rpm and 30G for the diameter of the syringe, because it was observed a great quantity of well-formed fibers without beads and no breakage. With some of the parameters not everything was varied cause the fibers produced under those parameters, were not visually well, and some defects were noticed. These parameters were further modified by different circumstances that affected the process, like the weather, therefore the speed was increased to 5500 rpm and the diameter of the syringes was increased to 27G, see table 4.

Table 4. Preliminary tests parameters.

Parameters					
N° Cycle	Solution Concentration	Cycle Time	Rpm	Syringe size	Humidity
1	15%	1 min	4500	27G	80%
2	15%	1 min	5000	30G	80%
3	15%	1 min	4000	30G	76%
4	15%	1 min	4000	30G	76%
5	15%	1 min	5000	30G	74%
6	15%	1 min	5500	30G	70%
7	15%	1 min	5500	30G	67%
8	15%	1 min	5000	25G	64%
9	15%	1 min	5500	27G	64%

The solutions were made in a ratio of 3:1 of Acetone and DMF respectively. The solvents were firstly mixed to then aggregate the PVDF polymer in a concentration of 15 % with respect to the total quantity of solution, to be magnetically stirred for 1 hour at 85°C at a constant speed. Then the resultant solution was left in stirring without heating to low the temperature of the solution until reaching an ambient temperature for their usage. In the case of the solutions where the nanofillers were added, the concentration

of BTO and G was established by information in the literature; the concentration of BTO and G was used in respect to the concentration of the polymer matrix. The nanofillers were firstly dispersed in the mix of solvents by magnetically stirring at a temperature of 50°C and at constant speed for 30 min, to then add the PVDF polymer and repeat the steps from the solution of the PVDF alone, this procedure is done for the elaboration of the samples that carry the nanofillers.

Table 5. Description of every solution that was used for the fabrication of piezoelectric sensors.

Key	Solution	Polymer concentration	Nanofiller	BaTiO <sub>3</sub> concentration	Graphene concentration	Mean diameter (µm)
A1	PVDF	15%	-	-	-	1.689
A2	BTO/PVDF	15%	BTO	15%	-	1.489
A3	G/PVDF	15%	G	-	0.05%	1.406
A4	BTO/G/PVDF	15%	BTO/G	15%	0.05%	1.122
A5	BTO/PVDF	15%	BTO	5%	-	1.045
A6	G/PVDF	15%	G	-	0.15%	1.197
A7	BTO/G/PVDF	15%	BTO/G	15%	0.15	1.272

Solutions with different concentrations of nanofillers are identified by the keys indicated in table 5, for ease of work with them. The concentration of the nanofillers were calculated in respect to the concentration of the polymeric matrix, for all samples.

### 3.5 Elaboration of fibers

The solution was injected into the spinneret to form the fibers. The needles used have an orifice diameter of 0.330 mm (27G), by the gelation property of the polymer, with low temperatures it was impossible to use a smaller size of needle. The rpm was set at 5500 rpm, because it showed an enhanced behavior at this speed. Then the fibers were collected for their assembly in the device.

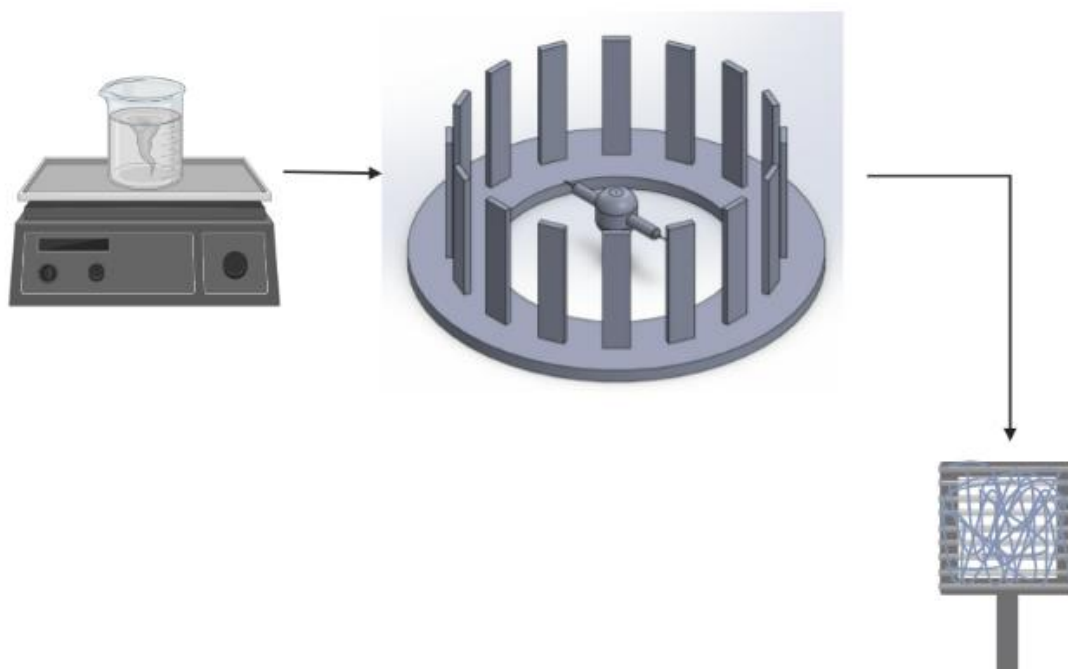


Figure 8. Diagram of the fiber synthesis.

### 3.6 Device Construction

As showed in fig 8 the fiber meshes were put between two copper foil tape electrodes and at the same time covered with polyamide tape (Kapton® tape) to protect the electrodes, the full device is sandwiched. Two copper wires are welded into the copper electrodes to pass the signals to the measuring equipment, an oscilloscope and a multimeter. The sensor is fabricated with an effective area of 3 cm x 3 cm (9 cm<sup>2</sup>). To avoid that both electrodes make contact between them, the electrodes were cut in a smaller size of 2.5cm x 2.5 cm.

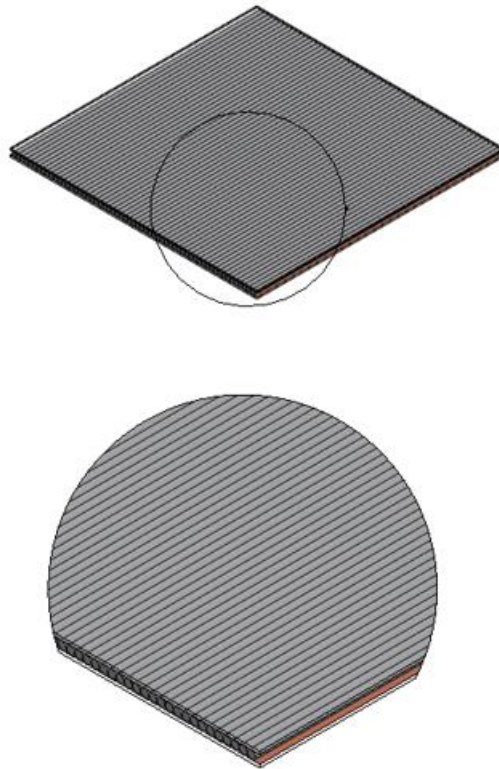


Figure 9. Device design.

### **3.7 Characterization**

The characteristics and parameters from each equipment used to characterize the materials used in this thesis project are presented in the next part.

#### **3.7.1 SEM Morphologic and Elemental distribution Characterization**

The morphology of the fiber meshes of the device was observed by scanning electron microscopy (SEM, Evo MA 25, Carl Zeiss, Oberkochen, Germany). The fibers were analyzed using an acceleration voltage of 10.00 kV and a working distance of 9.0 mm. The distribution of the materials is analyzed using an EDS detector (EDS, Bruker) at an accelerating voltage of 20 kV and a working distance of 9.3 mm. ImageJ software is utilized to process, analyze and measure different aspects from the SEM images.

#### **3.7.2 FTIR Composition Characterization**

The IR spectrum of the nanofiber meshes were analyzed in the equipment FTIR with the attenuated total reflectance (PerkinElmer, Frontier, Waltham, MA, USA) accessory. The samples were measured using a frequency range of 4000  $\text{cm}^{-1}$  to 400  $\text{cm}^{-1}$ , resolution of 4  $\text{cm}^{-1}$  and an average of 16 accumulated scans.

#### **3.7.3 TGA Thermal Characterization**

The thermogravimetric analysis (TGA) of the fiber meshes was carried out using a PerkinElmer analyzer (software Pyris 1), considering a temperature range between 30 °C to 700 °C and a heating rate of 10 °C/min. The nitrogen gas flow will be set at 20 mL/min. The initial weight of the samples was 5 mg. Samples are first discharged from electrostatic charges using an isolated mat.

### **3.7.4 XRD Structural Characterization**

The x-ray diffractometer (XRD) PANalytical analyzed the tests using slits of  $\frac{1}{4}$  to 1 at a voltage of 45 Kv with an amperage of 40 mA. It worked with a Cu  $\kappa\alpha$  radiation and a  $2\theta$  scanning range from  $5^\circ$  to  $90^\circ$ . Sample tests are covered with a thin film of gold, using sputtering.

### **3.7.5 Piezoelectric Characterization**

The electrical characterization was done using the impact tester (Charpy) that will be used to produce pressure in the device, a multimeter (Agilent) used in the mode of hold maximum peak to register the maximum voltage produced and an oscilloscope (Tektronix) that will be connected to the copper wires of the sensor to observe the shape of the signal that the sensor can generate when a mechanical force is applied to it. The pressure that is applied to the sensor is of 2.77 N with a speed of 3.46 m/s. The tool that is used to apply the force in the material in the Charpy machine, is covered with a protective cover to reduce the damage done to the device, the size of the impact area is of 2.2 cm x 1.8 cm.

## Chapter 4

### 4. Results and Discussion

#### 4.1 Barium Titanate Synthesis

The SEM images and the results were obtained using ImageJ, from the sol-gel method for nanoparticle fabrication are presented in figure 9, where the mean of the particle's size was observed, getting a result of 32 Nm, there are also present some agglomerates. Thus, the material has a good size for its usage as dopant in the polymeric matrix.

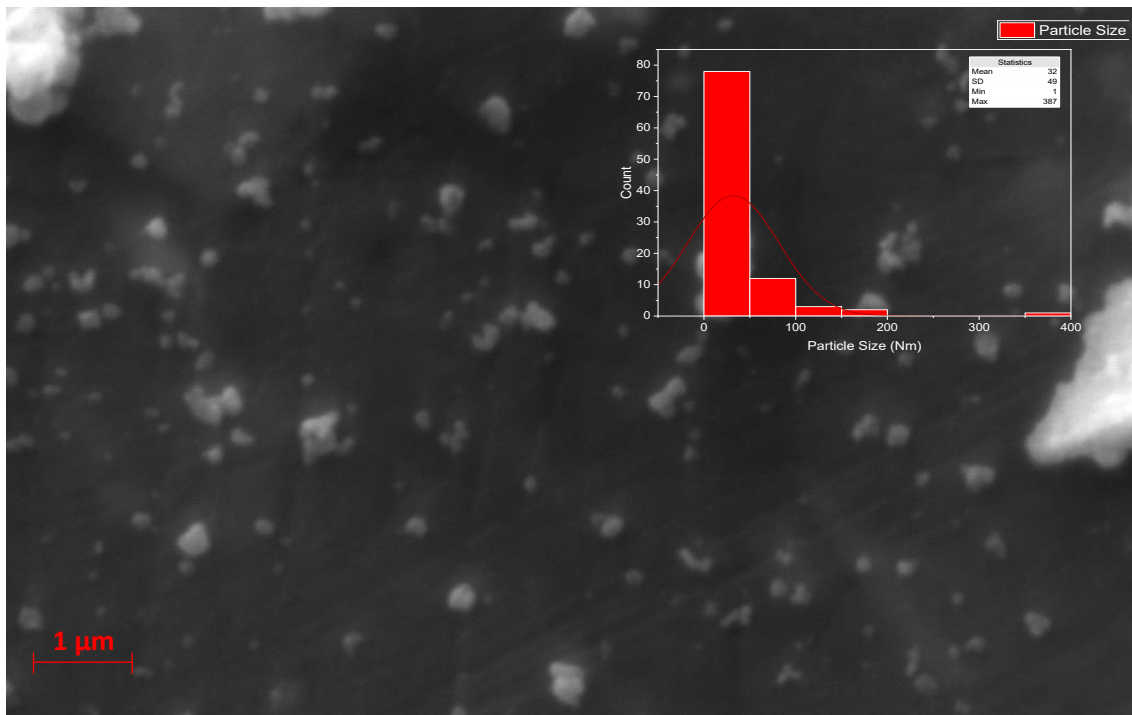


Figure 10. SEM image of BTO particles with a graph of the size of the particles.



XRD was performed on the material obtained from the sol-gel method, showing that the material presents the 99% of the phase desired comparing it with the crystallographic card 96-150-7758 that belongs to the “Match!” software. So, the resultant material from the sol-gel method is barium titanate with a perovskite structure. The diffraction pattern obtained from the nanoparticles elaborated for this project are in the angles  $2\theta$ : 22.26°, 31.6°, 38.98°, 45.28°, 51.03°, 56.21° and 65.83°, showing a similar pattern comparing it with the crystallographic card, the comparison of the diffractogram is presented in figure 10.

Also, the following planes were reported in the  $2\theta$ : 22.184° (100), 31.49° (110), 38.84° (111), 45.15° (200), 50.72° (210), 56.075° (211) and 65.711° angles in concordance with the JCPDS 05-0626 by Lazareví et al. 2009, Sabry et al. 2019 and Zhao et al. 2019 98–100.

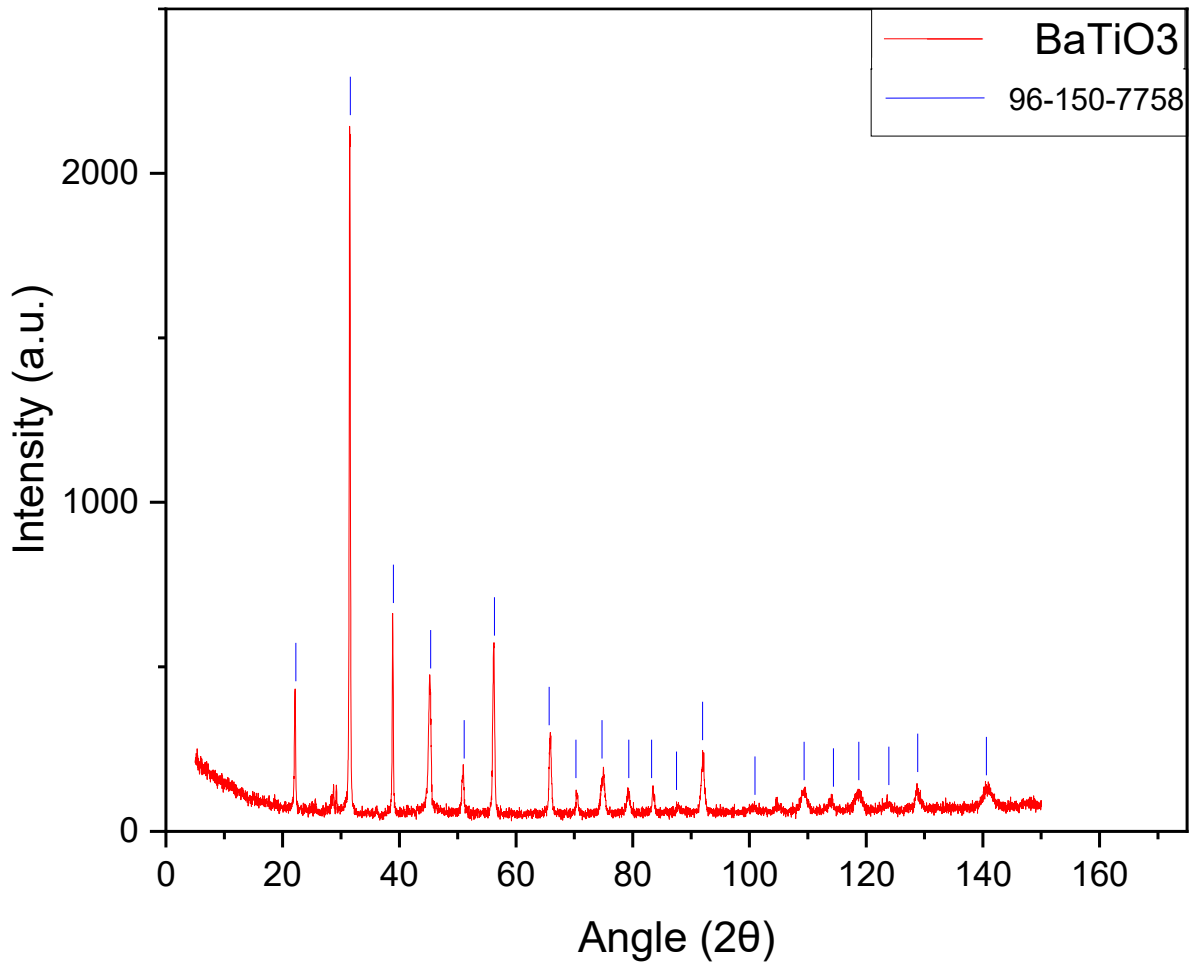


Figure 11. XRD Diffractogram of BTO.

## **4.2 Nanofiber Synthesis**

### **4.2.1 Morphologic Characterization**

SEM was used to examine the morphologies, diameters, chemical distributions, and compositions of PVDF nanofibers meshes, BTO-PVDF, G-PVDF and synergies with different concentration of dopants. Figure 11 shows that A1, A2, A3, A4, A5, A6, and A7 are the composites fibers meshes, which have a random orientation of the fibers and diameters of approximately 1  $\mu\text{m}$ , these conditions coincide with was reported by Rubaiya et al. 2021 and Ibtehaj et al. 2020 <sup>42,101</sup>. In the case of A1, the PVDF fibers show a smooth surface, that differentiates them from the rest of the fibers, because with the addition of nanofillers the fibers produced, presented a rough surface that help to promote the generation of voltage by the friction caused between the fibers with this surface <sup>81</sup>. Twenty fibers from each of the images were analyzed and measured to obtain the mean diameter of the fibers, a decrease in the diameter size, from the ones of pure PVDF with the ones with nanofillers can be noticed.

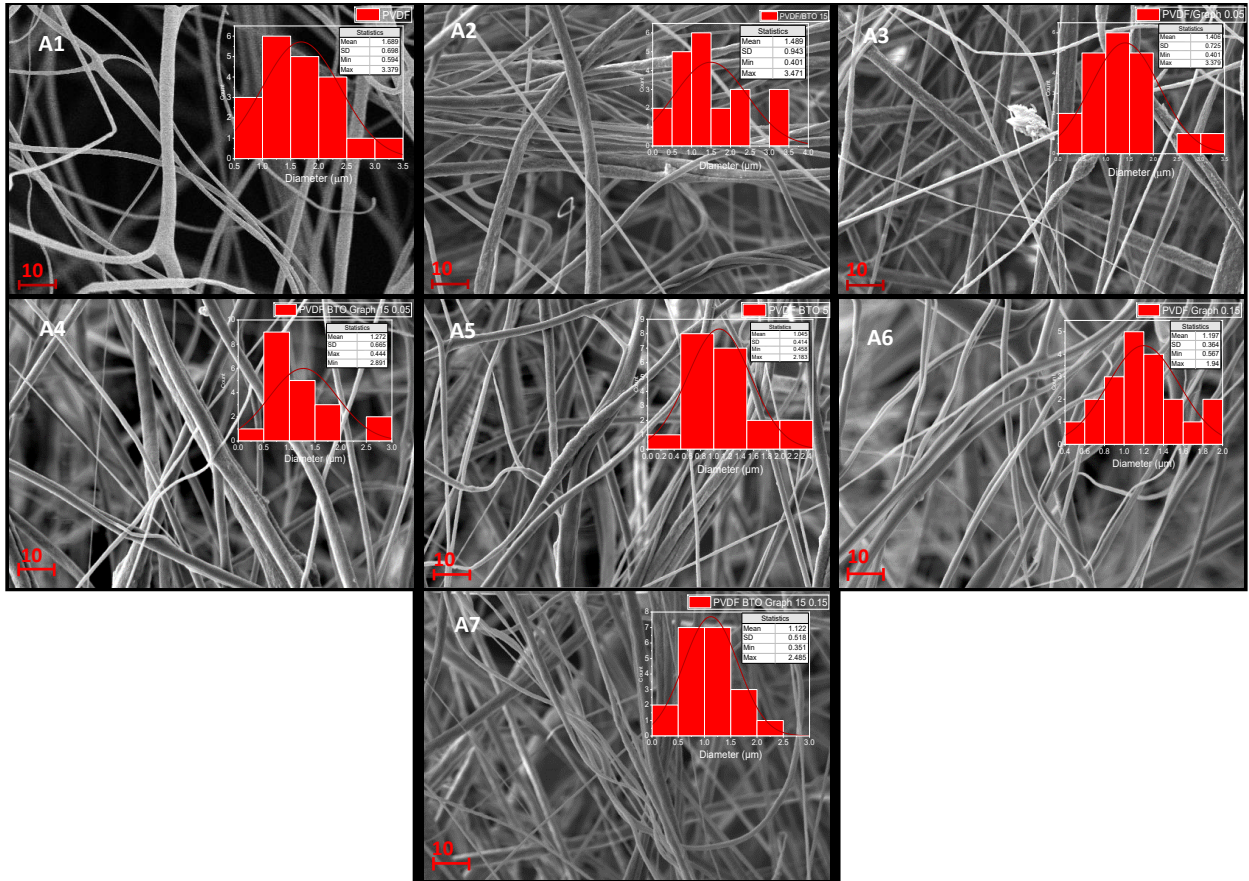


Figure 12. SEM images of the nanofibers for each composite with a graph for the representation of the mean diameter of the fibers. A1) PVDF, A2) BTO 15%/ PVDF, A3) G 0.05%/PVDF, A4) BTO 15%/G 0.05%/PVDF, A5) BTO 5%/PVDF, A6) G 0.15%/PVDF, A7) BTO 15%/G 0.15%/PVDF.

Energy dispersive spectroscopy (EDS) analysis was performed with a punctual test and a mapping to corroborate the presence of the desired elements of BTO on the synergy composite fibers meshes shown in figures 12, 13, and 14. From the figures we can observe that the elements that composed the BTO are distributed in the meshes, there are some agglomerates showed as more intense dots, but even though the BTO composite is evenly distributed. From the punctual test we can declare that there exists the presence of the material in the polymer fibers.

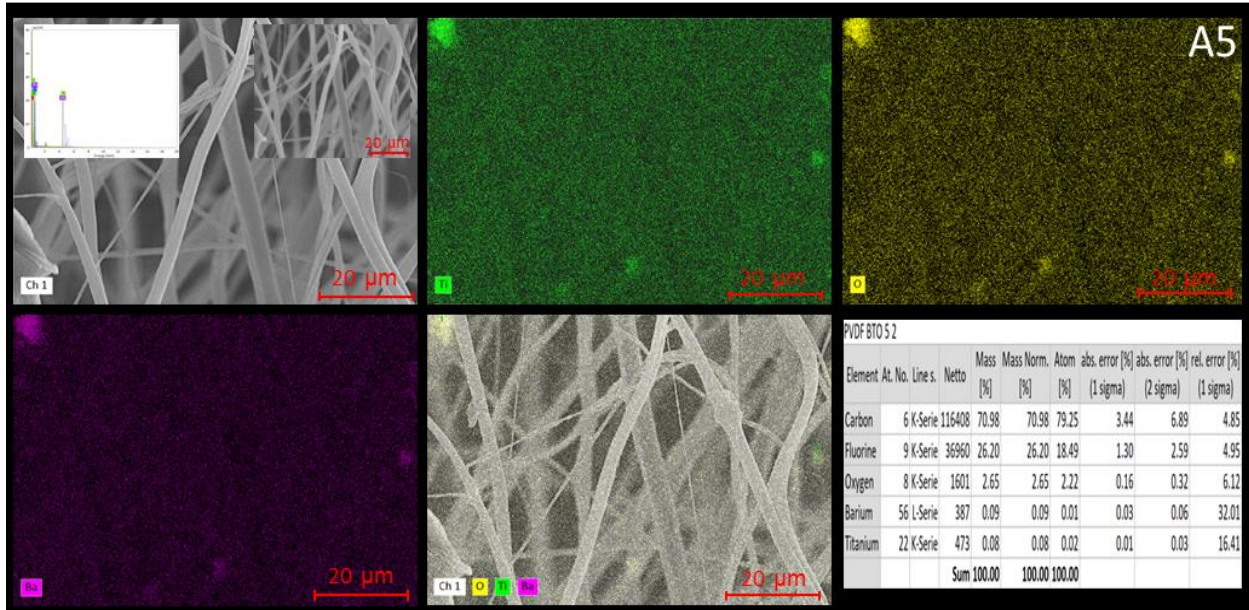


Figure 13. EDS images of the nanofibers for A5) BTO 5%/PVDF, we can observe the distribution of the material in the meshes of each element of the BTO, and a punctual test to observe the presence of the BTO in the meshes.

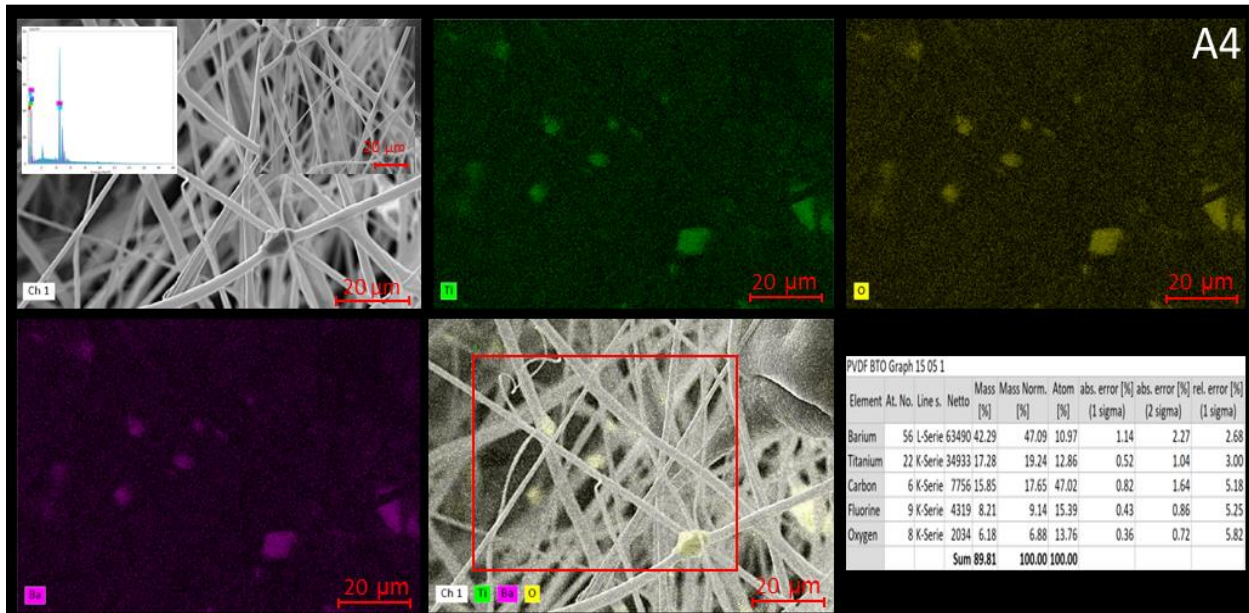


Figure 14. EDS images of the nanofibers for A4) BTO 15%/G 0.05%/PVDF, we can observe the distribution of the material in the meshes of each element of the BTO, and a punctual test to observe the presence of the BTO in the meshes.



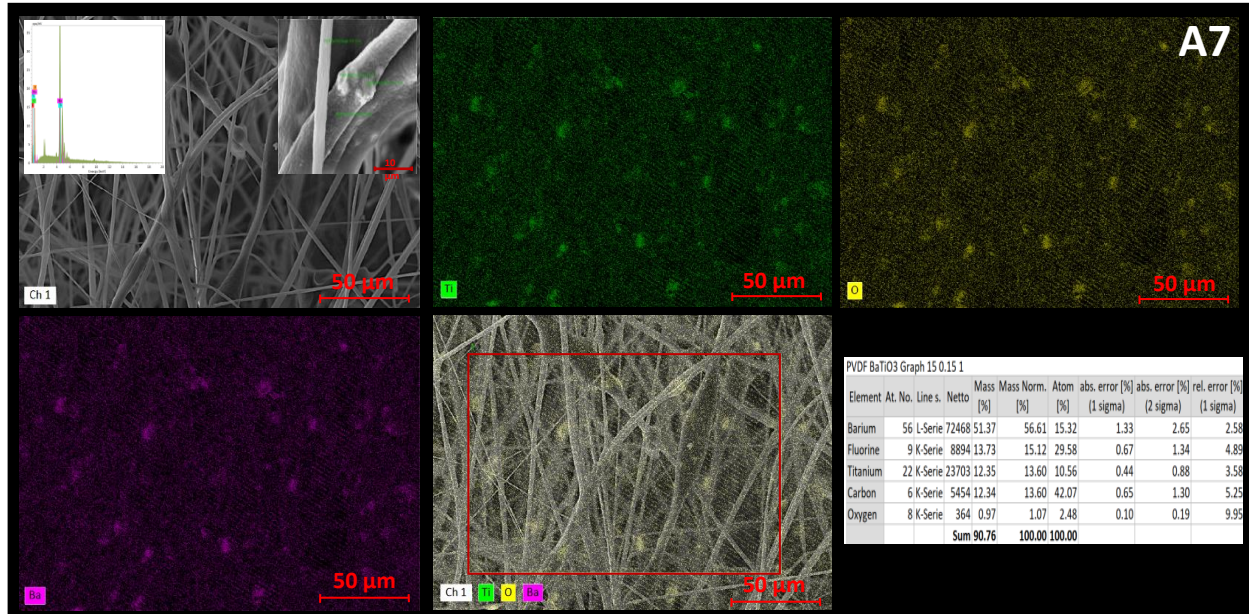


Figure 15. EDS images of the nanofibers for A7) BTO 15%/G 0.15%/PVDF, we can observe the distribution of the material in the meshes of each element of the BTO, and a punctual test to observe the presence of the BTO in the meshes.

#### 4.2.2 FTIR Composition Characterization

For the compositional characterization from FTIR the results that were obtained for both phases are presented in the figure 15 , where a change was observed in the signal emitted from the raw PVDF polymeric material where the  $\alpha$  phase is predominant changes after the synthesis process is applied to the material, diminishing the bands of  $\alpha$  phase and increasing the ones of  $\beta$  phase. The wavelenghts of the bands that belong to the  $\alpha$  phase are located at  $764\text{ cm}^{-1}$ ,  $796\text{ cm}^{-1}$  and  $976\text{ cm}^{-1}$  and the ones that belong to the  $\beta$  phase are in the bands  $840\text{ cm}^{-1}$ ,  $876\text{ cm}^{-1}$ ,  $1072\text{ cm}^{-1}$ ,  $1172\text{ cm}^{-1}$ ,  $1276\text{ cm}^{-1}$ , and  $1400\text{ cm}^{-1}$  <sup>24,42,48</sup>. The higher the vibration of the bands of each of the IR spectra indicates that the material presents more content of the desired phase, being able to identifacte that the solution with more content of  $\beta$  phase is observed in the sample A4, the sinergy solution of BTO and G at concentrations of 15 % and 0.05 % respectively.

Is also reported that the  $\alpha$  phase peaks corresponding to the  $765\text{ cm}^{-1}$  and the one at  $975\text{ cm}^{-1}$  where the spectra identifies the phenomena described by the vibrations is bending of  $\text{CF}_2$  and rocking of  $\text{CH}_2$  respectively. For the  $\beta$  phase at the peak of  $840\text{ cm}^{-1}$  the vibrations produced are for the phenomena of  $\text{CH}_2$  rocking,  $\text{CF}_2$  stretching and skeletal C–C stretching <sup>11</sup>.

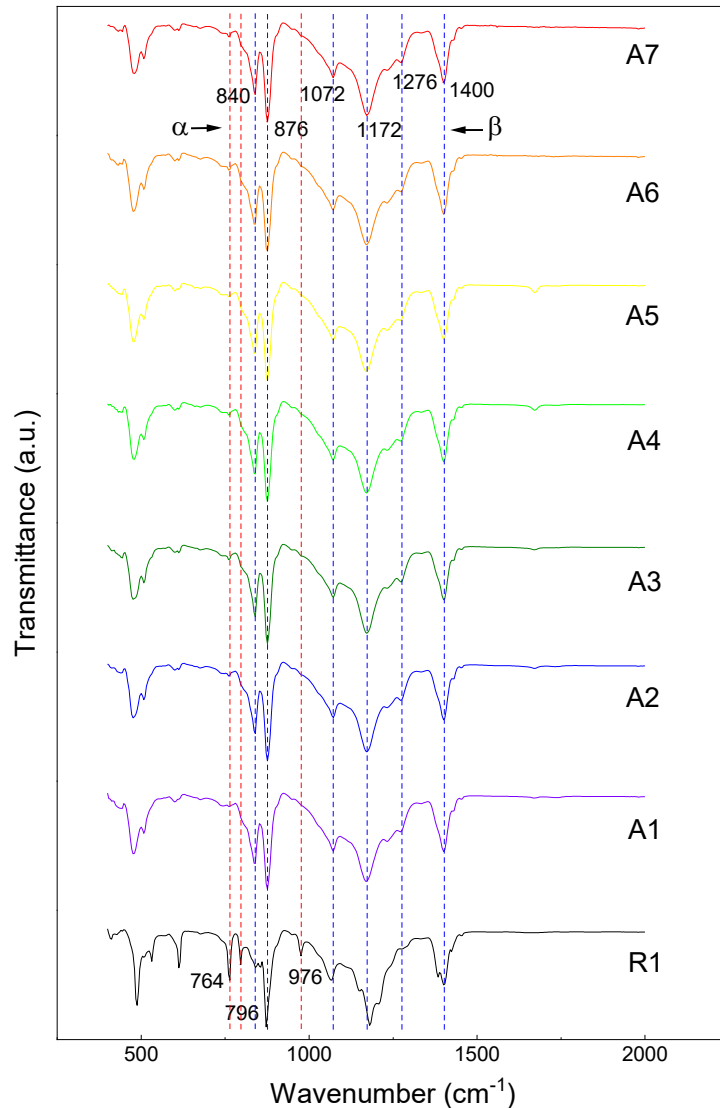


Figure 16. FTIR spectra from all the composites and the raw material. A1) PVDF, A2) BTO 15%/PVDF, A3) G 0.05%/PVDF, A4) BTO 15%/G 0.05%/PVDF, A5) BTO 5%/PVDF, A6) G 0.15%/PVDF, A7) BTO 15%/G 0.15%/PVDF.

The following equation, Eq. 3 that comprises the absorbance coefficients of the PVDF, one belonging to the  $\alpha$  phase and the other one to the  $\beta$  phase,  $k_{\alpha}$  and  $k_{\beta}$ , with values of  $6.1 \times 10^4 \text{ cm}^2 \text{ mol}^{-1}$  and  $7.7 \times 10^4 \text{ cm}^2 \text{ mol}^{-1}$  respectively, is used to calculate the  $\beta$  phase percentage in the composite materials by using the absorbance values obtained in the spectra.  $A_{\alpha}$  is the value of the characteristic  $\alpha$  phase wavelenght at  $763 \text{ cm}^{-1}$  and  $A_{\beta}$  is the value of the characteristic  $\beta$  phase wavelenght at  $840 \text{ cm}^{-1}$  <sup>42</sup>. From the values



obtained, it can be observed that all the samples with different concentration of fillers variates in a close range of  $\beta$  phase range of 4 units, where the best one is the synergy of BTO and G at 15 % and 0.15 % respectively. By the results obtained we can declare that this technique is good to promote the  $\beta$  phase formation in the PVDF, also the addition of the nanofillers and the mixture of solvents promote this formation.

(Eq.3)

$$F(\beta) = \frac{A_{\beta}}{\frac{k_{\beta}}{k_{\alpha}} A_{\alpha} + A_{\beta}} = \frac{A_{\beta}}{1.26 A_{\alpha} + A_{\beta}}$$

Table 6. Phase  $\beta$  percentage calculations from FTIR spectra.

Phase $\beta$ percentage				
Solution	$A_{\alpha}$	$A_{\beta}$	$\beta$	$\beta$ percentage
R1	0.1676	0.119	0.35999445	36.0%
A1	0.0233	0.1371	0.82336668	82.3%
A2	0.0225	0.1242	0.81388379	81.4%
A3	0.026	0.1206	0.78607911	78.6%
A4	0.0303	0.1652	0.81200293	81.2%
A5	0.0195	0.1106	0.81795808	81.8%
A6	0.0219	0.1062	0.79345949	79.3%
A7	0.0191	0.1176	0.82986477	83.0%

During the fabrication process and by the interaction of the material with the polar solvents, the molecular dipoles are rearranged forming the  $\beta$  phase with a TTTT conformation<sup>73</sup>. In the table 6, it can be observed the values obtained for the  $\beta$  phase percentage that is present in each of the synthesized materials. The material that presents the best  $\beta$  phase percentage is the synergy material in the sample A7) BTO 15%/G 0.15%/PVDF.

### 4.2.3 Thermal Characterization

From the thermogram was observed that with the addition of fillers the initial degradation temperature not changes between the pure fibers of PVDF material and the ones with added G, but the opposite effect occurs with the fibers that present the BTO material, presenting an increase in the initial degradation temperature. Therefore, offering more thermal stability in the samples that presents BTO <sup>57,102</sup>. TGA results are showed for the developed PVDF composite fibers A1, A2, A3, A4, A5, A6 and A7 samples in Figure 16. Temperature dependence shows one-step weight loss between 420°C-500°C with an inflection point around 480°C – 490°C with a loss in weight percentage of 65% for all the cases, a second drop is observed in the materials that present the BTO at a temperature around 560°C and 570°C that could be easily observed in the graph of the derivative see Figure 17. For the pure material and the composites that contains G at that temperature almost all the material has been degraded until nothing is left. The last step of the measurement is a thermoxidation because the gas is changed from nitrogen to oxygen, to completely reduce everything, but the BTO remains there because it is fabricated on higher temperatures.

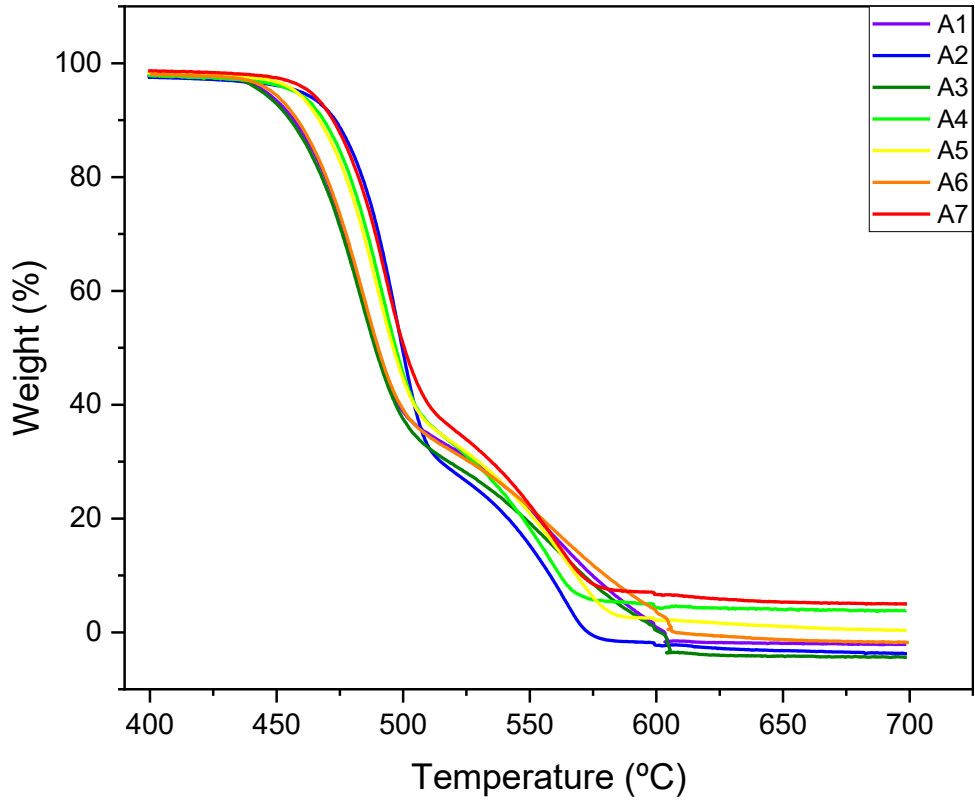


Figure 17. TGA Thermograms from all the samples. A1) PVDF, A2) BTO 15%/ PVDF, A3) G 0.05%/PVDF, A4) BTO 15%/G 0.05%/PVDF, A5) BTO 5%/PVDF, A6) G 0.15%/PVDF, A7) BTO 15%/G 0.15%/PVDF.

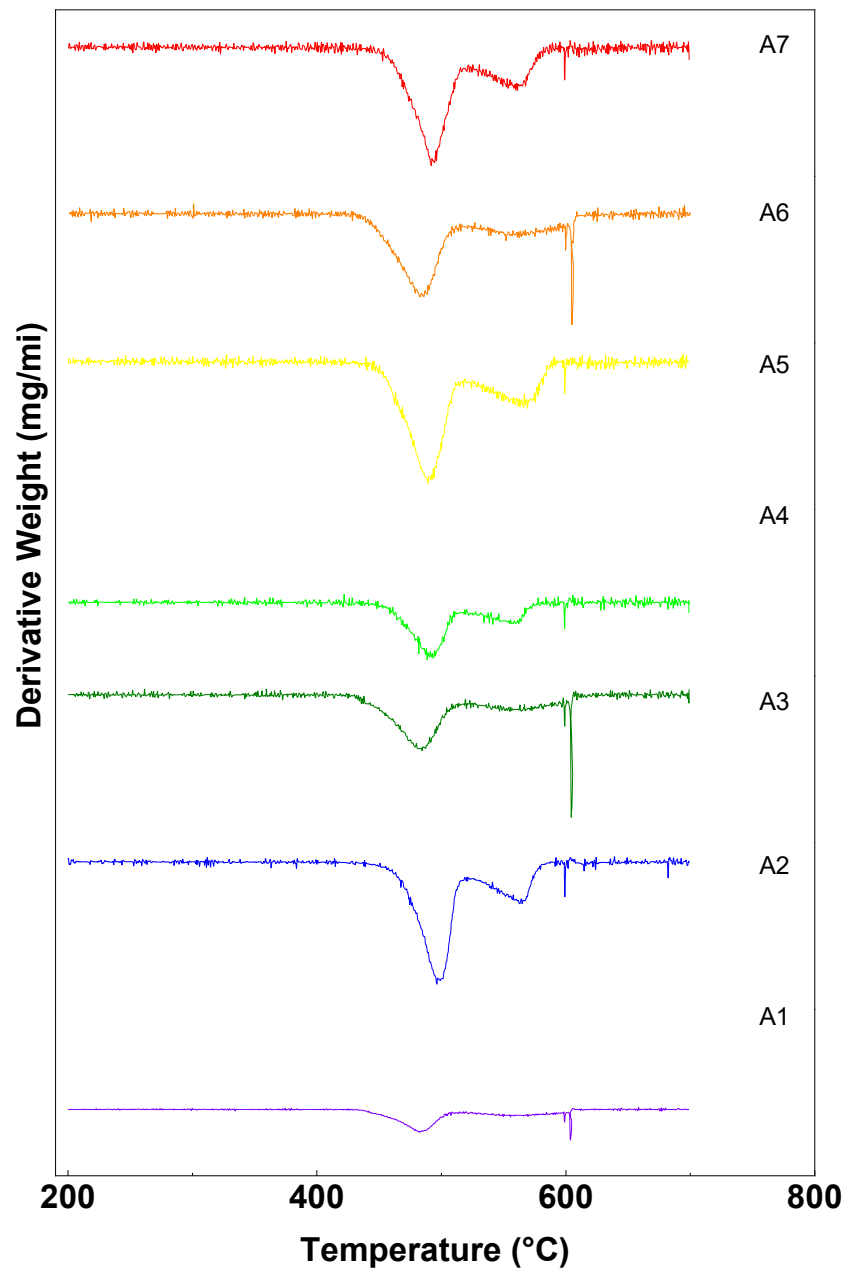


Figure 18. TGA Derivatives of the thermograms from all the samples. A1) PVDF, A2) BTO 15%/ PVDF, A3) G 0.05%/PVDF, A4) BTO 15%/G 0.05%/PVDF, A5) BTO 5%/PVDF, A6) G 0.15%/PVDF, A7) BTO 15%/G 0.15%/PVDF.

The maximum degradation temperature obtained from the derivate of the thermograms for each of the composites is presented in the Table 7 where an increase in the degradation temperature was observed, with an evident change in the cases that have BTO, as mentioned before. The most thermally stable is the composite A2 sample of PVDF with BTO at 15%, the other ones with BTO have similar behavior, but the ones that present G or does not have any filler have a worst behavior.

Table 7. Maximum degradation temperature.

<b>TGA maximum degradation temperature</b>	
<b>Solution</b>	<b>Temperature °C</b>
A1	482.54 °C
A2	497.25 °C
A3	483.32 °C
A4	491.56 °C
A5	489.80 °C
A6	484.11 °C
A7	492.35 °C

#### 4.2.4 Structural characterization

From the diffractogram was observed that the materials suffer a change in crystallinity after they are processed using the Forcespinning™ technique, therefore inducing a change of phase in the material are shown in the Figure 18. The planes that are representative for the  $\alpha$  phase are in the  $18.3^\circ$ ,  $19.8^\circ$  and  $26.6^\circ$  angles and the planes that represent the  $\beta$  phase are in the  $20.4^\circ$ ,  $36.5^\circ$  and  $40.2^\circ$  angles to samples elaborated for this thesis project but both phases tie with other researchers<sup>24,42,101</sup>. The diffraction at  $20.2^\circ$  is for the material that remained in the transition from the  $\alpha$  phase to the  $\beta$  phase<sup>22</sup>. The diffraction pattern of the G cannot be observed by the low content in the doped material in the A3 and A6 samples,<sup>100</sup>. It was observed that the diffractograms have a phase mixture that correspond to the presence of the BTO as dopant in the PVDF polymeric matrix. The planes that are attributed to the presence of BTO in the diffractograms of A2, A4, A5, A7 are present in the angles  $2\theta$ :  $31.6^\circ$ ,  $38.7^\circ$ ,  $45.13^\circ$ , and  $56.14^\circ$ .

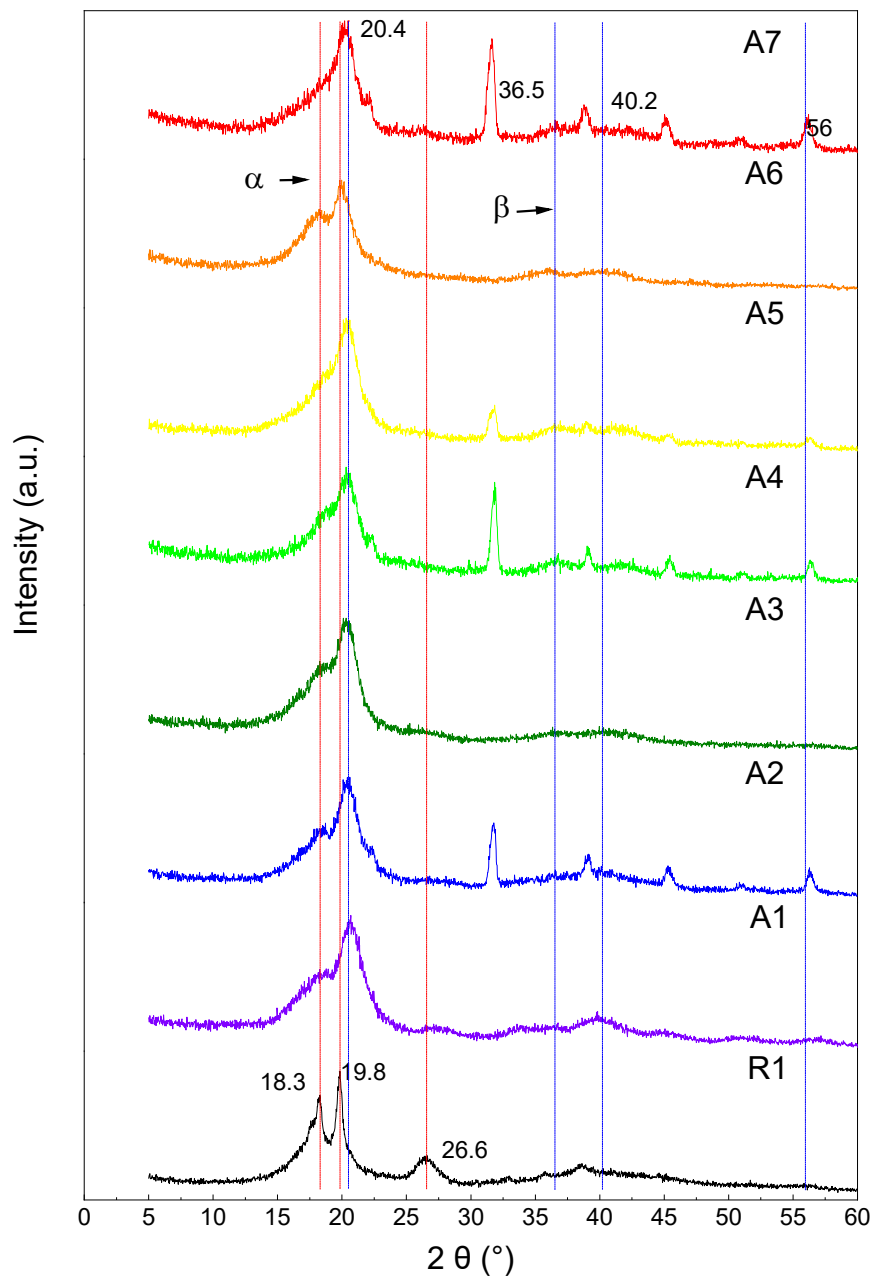


Figure 19. XRD Diffractogram of all the samples. A1) PVDF, A2) BTO 15%/ PVDF, A3) G 0.05%/PVDF, A4) BTO 15%/G 0.05%/PVDF, A5) BTO 5%/PVDF, A6) G 0.15%/PVDF, A7) BTO 15%/G 0.15%/PVDF.

#### 4.2.5 Piezoelectric characterization

Electrical response from the devices were evaluated using an electrometer with a function for holding the maximum voltage that is generated by using the Charpy (impact tester) on the sensor. The sensor that has the best performance between the 7 devices that were fabricated is the A2: BTO 15%/PVDF with a mean of 35.77 V<sub>oc</sub> generated by using 2.77 N. According to the Figures 19 and 20, the synergies made between the BTO/G/PVDF and the composites with just G are the ones with the worst performance between all the devices made, and the better ones, those with BTO as nanofiller doping. The voltage results are different in all samples.

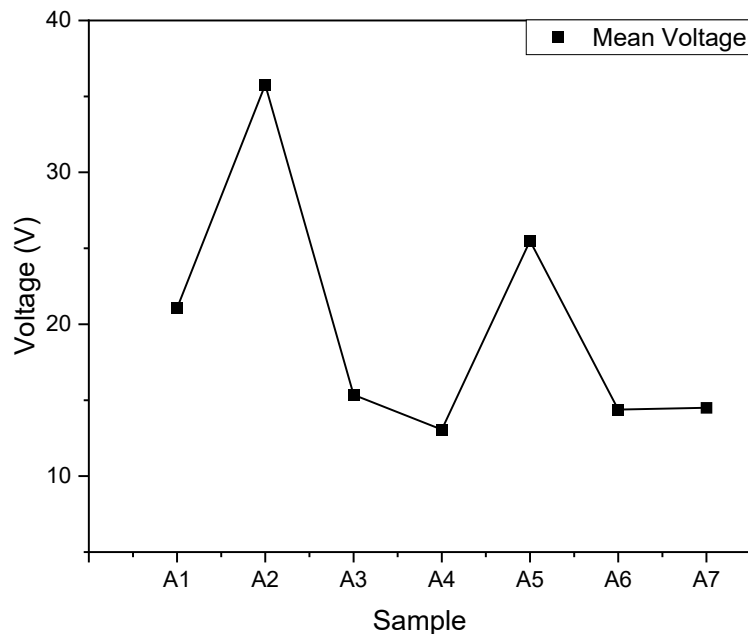


Figure 20. Device distribution by voltage output. A1) PVDF, A2) BTO 15%/ PVDF, A3) G 0.05%/PVDF, A4) BTO 15%/G 0.05%/PVDF, A5) BTO 5%/PVDF, A6) G 0.15%/PVDF, A7) BTO 15%/G 0.15%/PVDF.



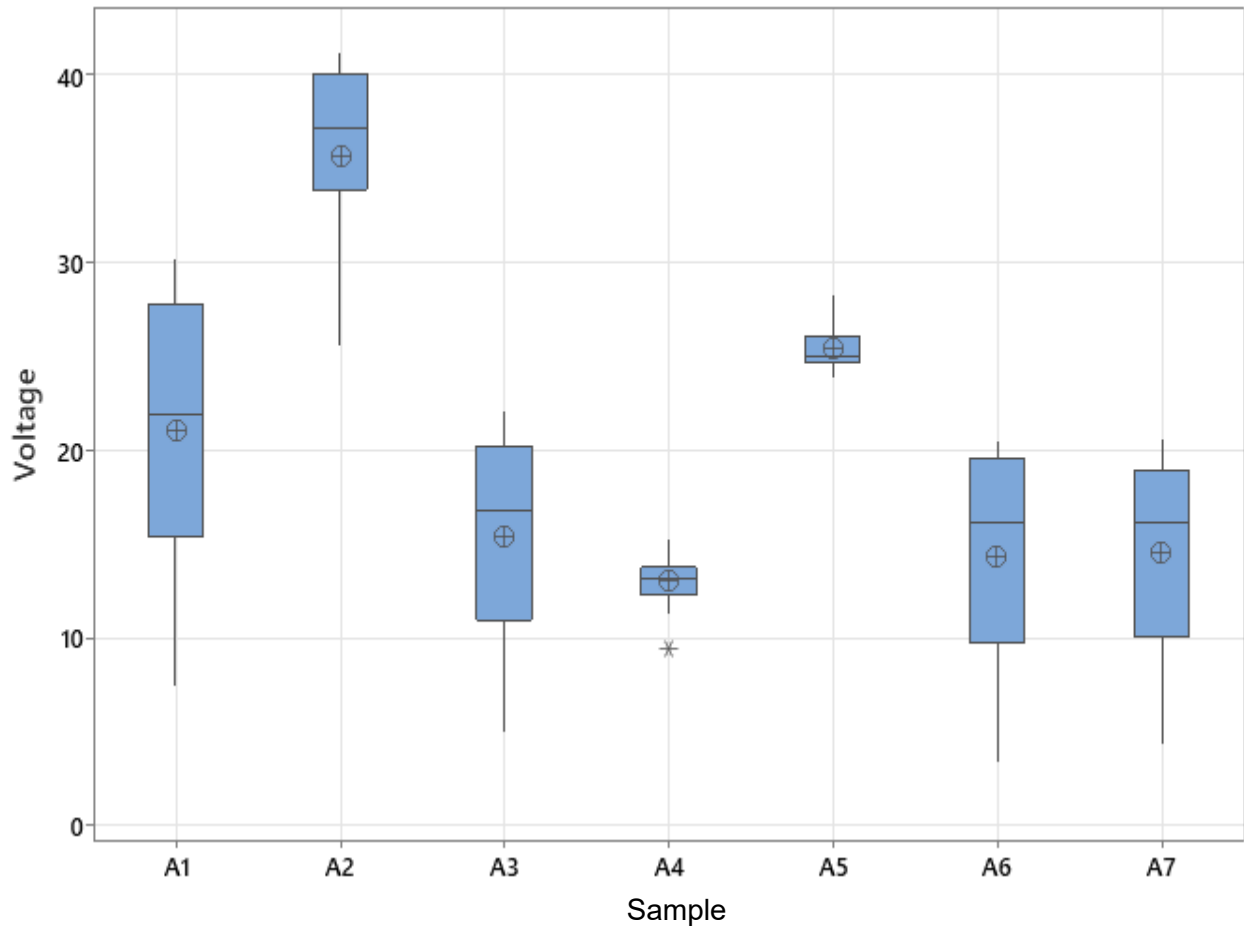


Figure 21. Boxplot of the voltage measured with the multimeter. A1) PVDF, A2) BTO 15%/PVDF, A3) G 0.05%/PVDF, A4) BTO 15%/G 0.05%/PVDF, A5) BTO 5%/PVDF, A6) G 0.15%/PVDF, A7) BTO 15%/G 0.15%/PVDF.

Table 8. Mean voltage produced by each device.

Mean Voltage (V)							
Solution	A1	A2	A3	A4	A5	A6	A7
Mean	21.06	35.77	15.35	13.06	25.49	14.38	14.50

Despite the material with the best phase  $\beta$  percentage was the A7, it is between the worst performance gadgets just producing 14.50 V mean. Therefore, other concentrations of G should be explored, to find the one with the best performance to agree with the phenomena explained in the article of Shi et al. where they found a synergy between the BTO and G. Results obtained in this thesis project are good, and they are reported in Table 8 from most of the devices elucidate that the sensors done are competitive to those ones published by other references <sup>23,42,56,81,101</sup>. There is a clear improvement in sensitivity in the materials with BTO, but by the contrary in the other cases there is a regression in these values for the other composites compared to the pure polymeric matrix PVDF device.

Sensitivity is determined by the equation 4, where V is for the mean maximum voltage produced by the device and F for the force applied to generate that voltage <sup>23</sup>. See table 9 with the sensitivity values.

**(Eq.4)**

$$Sensitivity = \frac{V}{F}$$

Table 9. Piezoelectric Sensitivity.

Sensitivity of the devices		
Sol	Mean Voltage	Sensitivity (V/N)
A1	21.06	7.60
A2	35.77	12.91
A3	15.35	5.54
A4	13.06	4.71
A5	25.49	9.20
A6	14.38	5.19
A7	14.50	5.23

For the determination of the piezoelectric coefficient,  $d_{33}$ , the samples that were exposed to this test are the ones with the best performance, A1, A2, and A5. The calculus made for the obtention of this coefficient is the following:

(Eq.5)

$$d_{33} = \frac{Q}{F} = \frac{C_m V_m}{F}$$

Where Q is denoted for the electric charge, that can be calculated by the capacitance (0.01  $\mu$ F) multiplied by the maximum voltage produced by the device, and F for the force exerted. In table 10 the values for the piezoelectric coefficient are shown.

Table 10. Piezoelectric Coefficient.

Piezoelectric coefficient	
Sample	$d_{33}$
A1	3.67 nC/N
A2	4.45 nC/N
A5	3.16 nC/N

The circuit elaborated for the measuring of the piezoelectric coefficient, is made of a rectifier bridge, where the piezoelectric device is connected, to then pass the electrical signal to a capacitor to generate a continuous signal, that can be measured for the calculus of the piezoelectric coefficient.

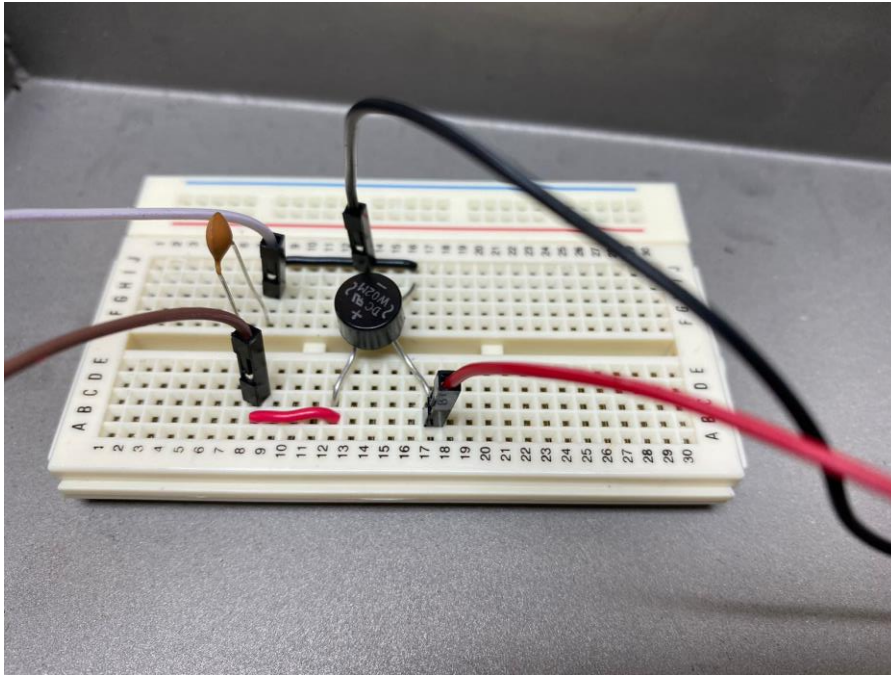


Figure 22. Electrical circuit for the piezoelectric coefficient.

To assess the behavior of the piezoelectric devices, the sensor with the best performance was exposed to different forces using different impact positions causing a difference in the voltage generation. The less the force exerted, the less voltage produced. The behavior is shown in figure 23. The value of the force exerted in each position are showed as follows:  $P_0 = 2.77\text{N}$ ,  $P_1 = 2.44\text{ N}$ ,  $P_2 = 2.27\text{ N}$ ,  $P_3 = 1.84\text{ N}$ , and  $P_4 = 1.57\text{ N}$ .

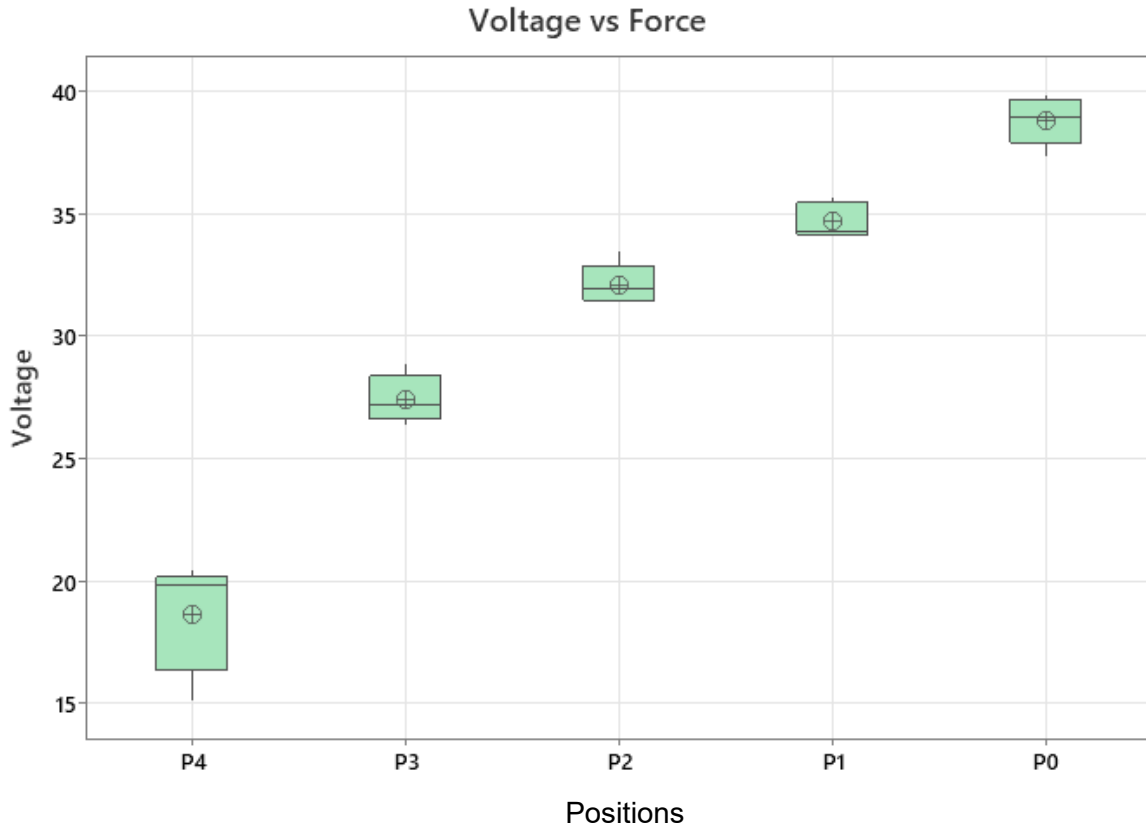


Figure 23. Voltage generated at different positions for sample A2) BTO 15%/PVDF. Value of the force for each position P0 = 2.77N, P1 = 2.44 N, P2 = 2.27 N, P3 = 1.84 N, and P4 = 1.57 N

The signal obtained from the oscilloscope has a sinusoidal shape, generated when the device is impacted with the Charpy machine. In the Figure 24, the shape visualized is the voltage generated in 5 tests.

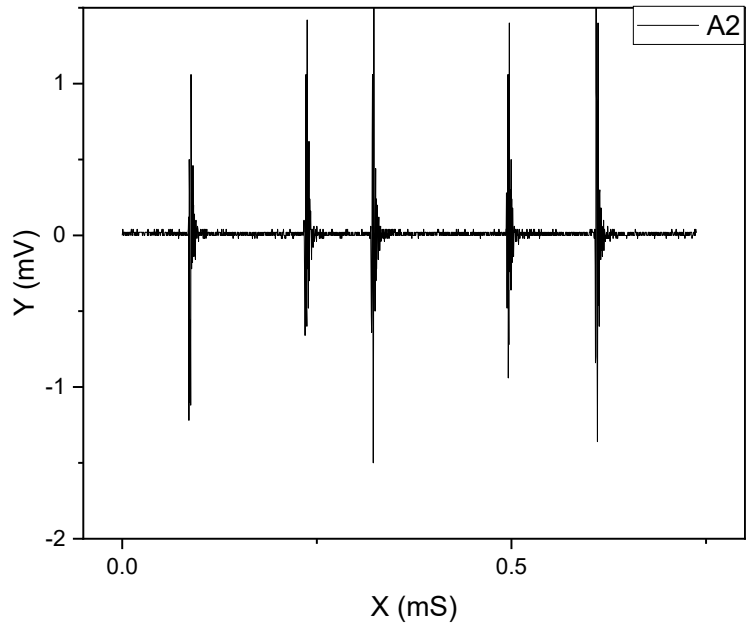


Figure 24. Shape for the signal obtained from the oscilloscope

In the figure 25, all the devices fabricated can be observed from all the composites, they are formed of the composite fibers with top and bottom electrodes of copper and over both electrodes Kapton tape to protect the sensors, and in figure 26 see the diagram of the piezoelectric characterization.

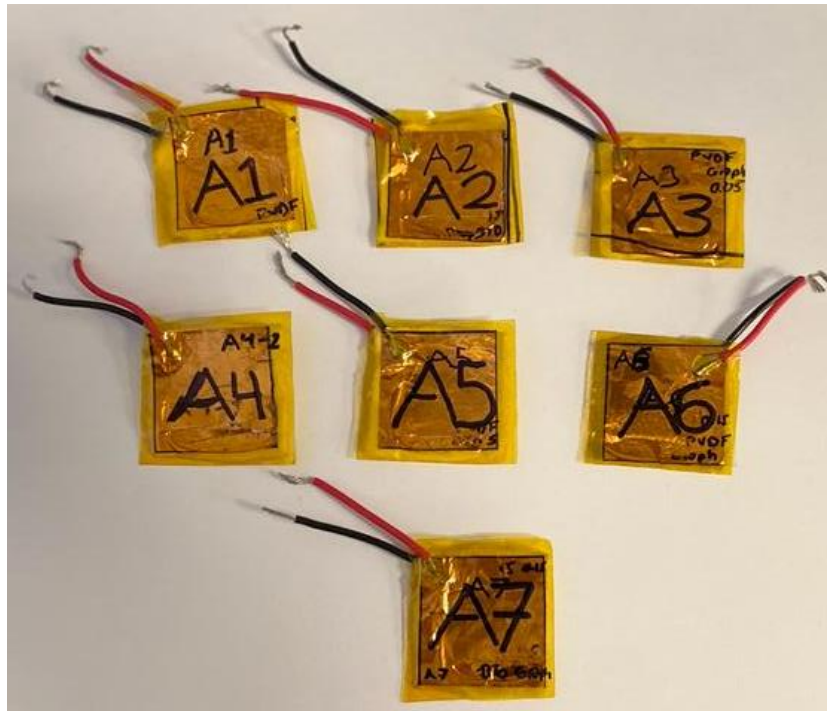


Figure 25. Devices fabricated from the different composites.

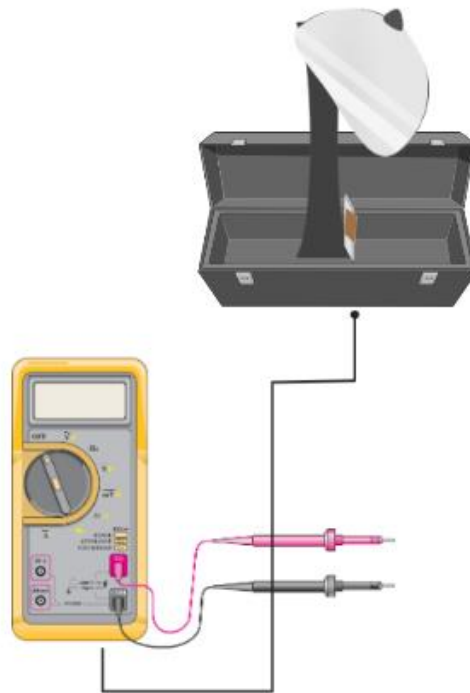


Figure 26. Diagram of the measuring process for the obtention of the output voltage.

In the table 11, it can be observed a comparison made between different piezoelectric devices with their test parameters and voltage produced, to see how the performance of the piezoelectric device is.



Table 11. Piezoelectric devices comparison

Authors	Polymeric Matrix	Nanofillers	Type of device	$\beta$ phase	Output Voltage	Measure way	d33	Durability
Experimental test	PVDF	BTO	Fibers	81.4%	35.77 V	External Force 2.77 N	4.45 nC/N	-
Eun et al. 2021. <sup>57</sup>	PVDF	MWCNT	Fibers	85%	0.62 V	Cycle of 2 Hz, bending tester in transverse direction	-	-
Ibtehaj et al. 2020. <sup>42</sup>	PVDF	None	Fibers	95.30 %	22 V	Repetitive vertical compression, 15 Hz, force of 4 N	-152 pC/N	10,000 cycles
Shi et al. 2018. <sup>24</sup>	PVDF	BTO/Graphene nanosheets	Fibers	91.10 %	11 V	Loading frequency of 2 Hz and a strain of 4 mm	-	1,800 cycles
Rubaiya et al. 2021. <sup>101</sup>	PVDF	ZGO	Fibers	-	Peak to peak voltage 172 V the maximum and 42 minimum	External force	-	-
Huang et al. 2021 <sup>14</sup>	PVDF-HFP	CQDs	Film	82.8%		Repeating different forces	22.6 pC/N	1000 s under 80 g

Liu et al. 2020 56	PVDF- TrFE	BZT-BCT	Fibers	-	13.01 V	Tapping 6N	-	5000 cycles
Yu et al. 2021 13	PVDF/GF F	BTS	Film		12.2V – 22.5 V	External Force 1 to 9N		5000 cycles under 50 N

*Chapter 4. Results and Discussion*

---

## Chapter 5

### 5. Conclusion

It is concluded that in this thesis project was used a novel approach to obtain the general purpose and each of the specific objectives projected were obtained. The BTO obtained by sol gel method, was confirmed with the crystallographic card 96-150-7758, using ImageJ it was determined that the particle size is around 32 nm. The commercial G nanopowder used, was of 2 – 10  $\mu\text{m}$  from 2 to 3 layers size. Both nanofillers were used as doping materials for PVDF polymeric matrix to generate fiber meshes by Forcespinning™ technique, but BTO particles were better than G without functionalizing. This was confirmed in the characterizations realized, SEM analysis shown fiber meshes randomly distributed with a diameter size around 1  $\mu\text{m}$ , and the EDS mapping images, also using a punctual test, confirmed us the presence of BTO nanofiller in the fiber meshes with agglomerations.

FTIR characterization showed visible changes in the spectra where more intense peaks can be observed in the bands that belongs to the  $\beta$  phase in comparison to the raw material.

TGA the maximum degradation temperature was obtained to determine which samples were the more thermally stable and the loss weight percentage that in samples with BTO confirmed the presence of this filler by the remains and XRD analysis confirmed us the presence of the planes of the  $\beta$  phase in the fiber meshes and the planes for the BTO for the perovskite type structure.

Finally, for the piezoelectric devices an Impact tester was used with a multimeter to record the voltage generated by all samples. Where the mean voltage generated was 35.77 V<sub>oc</sub> for the sample A2 were BTO nanoparticles were used as nanofillers and the devices with the poorer performance are the A3, A4, A6 and A7 devices where G was used as filler for synergies and as individual dopant in the PVDF polymeric matrix. Therefore, it is concluded that these materials can be used to produce piezoelectric devices that can function as sensors or nanogenerators with several applications in daily life, although they could be improved.

## 6. Future Work

- Change of polar solvents, DMF for DMSO, to test if the PVDF meshes have an increase in the  $\beta$  phase to promote the piezoelectric properties of the devices.
- Usage of PVDF co-polymers to promote better piezoelectric properties.
- Functionalization of G to obtain better results in the generation of  $\beta$  phase and increasing the voltage generation of piezoelectric devices.
- Integration of the piezoelectric device with a microcontroller to develop real applications that can be of usage
- Development of a station for piezoelectric characterization where devices can be tested easily for the obtention of the parameters.
- Obtention of piezoelectric coefficient

## Bibliography

1. Zhu, M., Yi, Z., Yang, B. & Lee, C. Making use of nanoenergy from human – Nanogenerator and self-powered sensor enabled sustainable wireless IoT sensory systems. *Nano Today* vol. 36 (2021).
2. Atzori, L., Iera, A. & Morabito, G. The Internet of Things: A survey. *Computer Networks* 54, 2787–2805 (2010).
3. Zanella, A., Bui, N., Castellani, A., Vangelista, L. & Zorzi, M. Internet of things for smart cities. *IEEE Internet of Things Journal* 1, 22–32 (2014).
4. Zhao, Z., Dai, Y., Dou, S. X. & Liang, J. Flexible nanogenerators for wearable electronic applications based on piezoelectric materials. *Materials Today Energy* vol. 20 (2021).
5. Al-Fuqaha, A., Guizani, M., Mohammadi, M., Aledhari, M. & Ayyash, M. Internet of Things: A Survey on Enabling Technologies, Protocols, and Applications. *IEEE Communications Surveys and Tutorials* 17, 2347–2376 (2015).
6. Postolache, O. A., Sazonov, E. & Mukhopadhyay, S. C. Sensors for the Internet of things. in *Sensors in the Age of Internet of Things - Technologies and Applications* (2019).
7. Khoshmanesh, F., Thurgood, P., Pirogova, E., Nahavandi, S. & Baratchi, S. Wearable sensors: At the frontier of personalised health monitoring, smart prosthetics and assistive technologies. *Biosensors and Bioelectronics* 176, 112946 (2021).
8. Zhou, H. *et al.* Stretchable piezoelectric energy harvesters and self-powered sensors for wearable and implantable devices. *Biosensors and Bioelectronics* 168, 112569 (2020).
9. Lu, B. *et al.* Ultra-flexible Piezoelectric Devices Integrated with Heart to Harvest the Biomechanical Energy. *Scientific Reports* 5, (2015).
10. Shawon, S. M. A. Z. *et al.* Surface modified hybrid ZnSnO<sub>3</sub> nanocubes for enhanced piezoelectric power generation and wireless sensory application. *Nano Energy* 92, 106653 (2022).
11. Yang, T. *et al.* Hierarchically structured PVDF/ZnO core-shell nanofibers for self-powered physiological monitoring electronics. *Nano Energy* 72, 104706 (2020).
12. Lee, S. *et al.* Super-flexible nanogenerator for energy harvesting from gentle wind and as an active deformation sensor. *Advanced Functional Materials* 23, 2445–2449 (2013).
13. Yu, D. *et al.* Superflexible and Lead-Free Piezoelectric Nanogenerator as a Highly Sensitive Self-Powered Sensor for Human Motion Monitoring. *Nano-Micro Letters* 13, (2021).

14. Huang, P. *et al.* Carbon quantum dots inducing formation of  $\beta$  phase in PVDF-HFP to improve the piezoelectric performance. *Sensors and Actuators, A: Physical* 330, 112880 (2021).
15. Hu, Y. & Wang, Z. L. Recent progress in piezoelectric nanogenerators as a sustainable power source in self-powered systems and active sensors. *Nano Energy* 14, 3–14 (2014).
16. Mokhtari, F., Azimi, B., Salehi, M., Hashemikia, S. & Danti, S. Recent advances of polymer-based piezoelectric composites for biomedical applications. *Journal of the Mechanical Behavior of Biomedical Materials* 122, 104669 (2021).
17. Rastegar, J. D. H. S. Mechanical-to-Electrical Energy Conversion Transducers. in *Energy Harvesting for Low-Power Autonomous Devices and Systems* (2017).
18. Lee, S. *et al.* Ultrathin nanogenerators as self-powered/active skin sensors for tracking eye ball motion. *Advanced Functional Materials* 24, 1163–1168 (2014).
19. Parangusan, H., Bhadra, J. & Al-Thani, N. Flexible piezoelectric nanogenerator based on [P(VDF-HFP)]/ PANI-ZnS electrospun nanofibers for electrical energy harvesting. *Journal of Materials Science: Materials in Electronics* 32, 6358–6368 (2021).
20. Ma, W. *et al.* Piezoelectricity in Multilayer Black Phosphorus for Piezotronics and Nanogenerators. *Advanced Materials* 32, (2020).
21. Issa, A., Al-Maadeed, M., Luyt, A., Ponnamma, D. & Hassan, M. Physico-Mechanical, Dielectric, and Piezoelectric Properties of PVDF Electrospun Mats Containing Silver Nanoparticles. *C (Basel)* 3, 30 (2017).
22. Liu, L., Fu, W., Wang, L., Tian, H. & Shan, X. Piezoelectricity of PVDF composite film doped with dopamine coated nano-TiO<sub>2</sub>. *Journal of Alloys and Compounds* 885, 160829 (2021).
23. Chamankar, N., Khajavi, R., Yousefi, A. A., Rashidi, A. & Golestanifard, F. A flexible piezoelectric pressure sensor based on PVDF nanocomposite fibers doped with PZT particles for energy harvesting applications. *Ceramics International* 46, 19669–19681 (2020).
24. Shi, K., Sun, B., Huang, X. & Jiang, P. Synergistic effect of graphene nanosheet and BaTiO<sub>3</sub> nanoparticles on performance enhancement of electrospun PVDF nanofiber mat for flexible piezoelectric nanogenerators. *Nano Energy* 52, 153–162 (2018).
25. Ham, S. S. *et al.* Kinetic motion sensors based on flexible and lead-free hybrid piezoelectric composite energy harvesters with nanowires-embedded electrodes for detecting articular movements. *Composites Part B: Engineering* 212, (2021).
26. Fuh, Y. K., Lee, S. C. & Tsai, C. Y. Application of Highly flexible self-powered sensors via sequentially deposited piezoelectric fibers on printed circuit board for wearable electronics devices. *Sensors and Actuators, A: Physical* 268, 148–154 (2017).
27. Eom, K. *et al.* Engineering crystal phase of Nylon-11 films for ferroelectric device and piezoelectric sensor. *Nano Energy* 88, (2021).

28. Tao, Z. *et al.* Diphenylalanine-based degradable piezoelectric nanogenerators enabled by polylactic acid polymer-assisted transfer. *Nano Energy* 88, (2021).
29. Wang, X., Yue, O., Liu, X., Hou, M. & Zheng, M. A novel bio-inspired multi-functional collagen aggregate based flexible sensor with multi-layer and internal 3D network structure. *Chemical Engineering Journal* 392, (2020).
30. Kaliannagounder, V. K. *et al.* Remotely controlled self-powering electrical stimulators for osteogenic differentiation using bone inspired bioactive piezoelectric whitlockite nanoparticles. *Nano Energy* 85, (2021).
31. Lee, B. Y. *et al.* Virus-based piezoelectric energy generation. *Nature Nanotechnology* 7, 351–356 (2012).
32. Wu, Y., Ma, Y., Zheng, H. & Ramakrishna, S. Piezoelectric materials for flexible and wearable electronics: A review. *Materials and Design* vol. 211 (2021).
33. Banerjee, S., Bairagi, S. & Wazed Ali, S. A critical review on lead-free hybrid materials for next generation piezoelectric energy harvesting and conversion. *Ceramics International* 47, 16402–16421 (2021).
34. Li, L., Xu, J., Liu, J. & Gao, F. Recent progress on piezoelectric energy harvesting: structures and materials. *Advanced Composites and Hybrid Materials* vol. 1 478–505 (2018).
35. Sezer, N. & Koç, M. A comprehensive review on the state-of-the-art of piezoelectric energy harvesting. *Nano Energy* vol. 80 (2021).
36. Lu, L., Ding, W., Liu, J. & Yang, B. Flexible PVDF based piezoelectric nanogenerators. *Nano Energy* 78, 105251 (2020).
37. Kalimuldina, G. *et al.* A review of piezoelectric pvdf film by electrospinning and its applications. *Sensors (Switzerland)* vol. 20 1–42 (2020).
38. Alhassan, Z. A., Burezq, Y. S., Nair, R. & Shehata, N. Polyvinylidene difluoride piezoelectric electrospun nanofibers: Review in synthesis, fabrication, characterizations, and applications. *Journal of Nanomaterials* vol. 2018 (2018).
39. Ebnasajjad, S. Introduction to Fluoropolymers. in *Applied Plastics Engineering Handbook* 55–71 (Elsevier, 2017). doi:10.1016/B978-0-323-39040-8.00003-1.
40. Yan, J. *et al.* Performance enhancements in poly(vinylidene fluoride)-based piezoelectric nanogenerators for efficient energy harvesting. *Nano Energy* vol. 56 662–692 (2019).
41. Ameduri, B. S. H. Commercial Synthesis and Applications of Poly(Vinylidene Fluoride). in *Fluorinated Polymers* vol. 2 Applications (Royal Society of Chemistry, 2017).
42. Ibtehaj, K., Hj Jumali, M. H. & Al-Bati, S. A novel facile preparation method of self-polarized Poly(vinylidene fluorides) nanofiber for high-performance piezoelectric nanogenerator. *Polymer (Guildf)* 208, 122956 (2020).



43. Tao, M. mi, Liu, F., Ma, B. rong & Xue, L. xin. Effect of solvent power on PVDF membrane polymorphism during phase inversion. *Desalination* 316, 137–145 (2013).
44. Gee, S., Johnson, B. & Smith, A. L. Optimizing electrospinning parameters for piezoelectric PVDF nanofiber membranes. *Journal of Membrane Science* 563, 804–812 (2018).
45. Russo, F. *et al.* Innovative poly (Vinylidene fluoride) (PVDF) electrospun nanofiber membrane preparation using DMSO as a low toxicity solvent. *Membranes (Basel)* 10, (2020).
46. He, Z., Rault, F., Lewandowski, M., Mohsenzadeh, E. & Salaün, F. Electrospun PVDF nanofibers for piezoelectric applications: A review of the influence of electrospinning parameters on the  $\beta$  phase and crystallinity enhancement. *Polymers* vol. 13 1–23 (2021).
47. Zhang, H. *et al.* Graphene-enabled wearable sensors for healthcare monitoring. *Biosensors and Bioelectronics* 197, 113777 (2022).
48. Faraz, M., Singh, H. H. & Khare, N. A Progressive Strategy for Harvesting Mechanical Energy using Flexible PVDF-rGO-MoS<sub>2</sub> nanocomposites film-based Piezoelectric Nanogenerator. *Journal of Alloys and Compounds* 161840 (2021) doi:10.1016/j.jallcom.2021.161840.
49. Sarkar, K. *et al.* Electrospinning to Forcespinning™. *Materials Today* 13, 12–14 (2010).
50. Vazquez, B., Vasquez, H. & Lozano, K. Preparation and characterization of polyvinylidene fluoride nanofibrous membranes by forcespinning™. *Polymer Engineering & Science* 52, 2260–2265 (2012).
51. Hernandez, C. *et al.* High pressure responsive luminescence of flexible Eu<sup>3+</sup> doped PVDF fibrous mats. *Journal of Materials Science and Technology* 66, 103–111 (2021).
52. Hernandez, C. *et al.* Performance evaluation of Ce<sup>3+</sup> doped flexible PVDF fibers for efficient optical pressure sensors. *Sensors and Actuators, A: Physical* 298, 111595 (2019).
53. Valdez, M., Gupta, S. K., Lozano, K. & Mao, Y. ForceSpun polydiacetylene nanofibers as colorimetric sensor for food spoilage detection. *Sensors and Actuators, B: Chemical* 297, 126734 (2019).
54. Bouaaliouat, O. *et al.* Forcespun metal oxide ultrafine tubes for hazardous gas monitoring. in *Materials Today: Proceedings* vol. 27 3124–3131 (2020).
55. Beringer, L. T. *et al.* An electrospun PVDF-TrFe fiber sensor platform for biological applications. *Sensors and Actuators, A: Physical* 222, 293–300 (2015).
56. Liu, J. *et al.* Flexible and lead-free piezoelectric nanogenerator as self-powered sensor based on electrospinning BZT-BCT/P(VDF-TrFE) nanofibers. *Sensors and Actuators, A: Physical* 303, 111796 (2020).

57. Eun, J. H., Sung, S. M., Kim, M. S., Choi, B. K. & Lee, J. S. Effect of MWCNT content on the mechanical and piezoelectric properties of PVDF nanofibers. *Materials and Design* 206, 109785 (2021).
58. Postolache, Octavian Adrian; Sazonov, Edward; Mukhopadhyay, S. C. Sensors for the Internet of things. in *Sensors in the Age of the Internet of Things: Technologies and applications* (Institution of Engineering and Technology, 2019).
59. Frank, Randy. Smart Sensor Basics. in *Understanding Smart Sensors* (Artech House, 2013).
60. Wang, Z. L. Toward self-powered sensor networks. *Nano Today* 5, 512–514 (2010).
61. Paladiya, C. & Kiani, A. Nano structured sensing surface: Significance in sensor fabrication. *Sensors and Actuators, B: Chemical* 268, 494–511 (2018).
62. Kenny, T. & Kester, W. Sensor Fundamentals. in *Sensor Technology Handbook* 1–20 (2005). doi:10.1016/B978-075067729-5/50041-0.
63. Velez, F. J. & Miyandoab, F. D. Wearables Medical Technologies and Devices, Networks and Frequency Bands. in *Wearable Technologies and Wireless Body Sensor Networks for Healthcare* (Institution of Engineering and Technology, 2019).
64. Velez, F. J. M. F. D. Implementation study of wearable sensors for human activity recognition systems. in *Wearable Technologies and Wireless Body Sensor Networks for Healthcare* (Institution of Engineering and Technology, 2019).
65. Sarker, M. R. *et al.* Review of piezoelectric energy harvesting system and application of optimization techniques to enhance the performance of the harvesting system. *Sensors and Actuators, A: Physical* vol. 300 (2019).
66. Singh, B. *et al.* Recent advances, challenges, and prospects of piezoelectric materials for self-charging supercapacitor. *Journal of Energy Storage* (2021) doi:10.1016/j.est.2021.103547.
67. Hao, J., Li, W., Zhai, J. & Chen, H. Progress in high-strain perovskite piezoelectric ceramics. *Materials Science and Engineering R: Reports* vol. 135 1–57 (2019).
68. Wu, N., Bao, B. & Wang, Q. Review on engineering structural designs for efficient piezoelectric energy harvesting to obtain high power output. *Engineering Structures* 235, (2021).
69. Rathod, V. T. A review of acoustic impedance matching techniques for piezoelectric sensors and transducers. *Sensors (Switzerland)* vol. 20 1–65 (2020).
70. Li, Y. *et al.* Multilayer assembly of electrospun/electrosprayed PVDF-based nanofibers and beads with enhanced piezoelectricity and high sensitivity. *Chemical Engineering Journal* 388, (2020).

71. Ghosh, S. K. & Mandal, D. Synergistically enhanced piezoelectric output in highly aligned 1D polymer nanofibers integrated all-fiber nanogenerator for wearable nano-tactile sensor. *Nano Energy* 53, 245–257 (2018).
72. Zaarour, B., Zhu, L. & Jin, X. Controlling the surface structure, mechanical properties, crystallinity, and piezoelectric properties of electrospun PVDF nanofibers by maneuvering molecular weight. *Soft Materials* 17, 181–189 (2019).
73. Li, X., Wang, Y., He, T., Hu, Q. & Yang, Y. Preparation of PVDF flexible piezoelectric film with high  $\beta$ -phase content by matching solvent dipole moment and crystallization temperature. *Journal of Materials Science: Materials in Electronics* 30, 20174–20180 (2019).
74. Raghavan, B., Soto, H. & Lozano, K. *Fabrication of Melt Spun Polypropylene Nanofibers by Forcespinning*. vol. 8 <http://www.jeffjournal.org>.
75. Padron, S., Fuentes, A., Caruntu, D. & Lozano, K. Experimental study of nanofiber production through forcespinning. *Journal of Applied Physics* 113, (2013).
76. Barhoum, A. *et al.* Review on Natural, Incidental, Bioinspired, and Engineered Nanomaterials: History, Definitions, Classifications, Synthesis, Properties, Market, Toxicities, Risks, and Regulations. *Nanomaterials* 12, (2022).
77. Kolahalam, L. A. *et al.* Review on nanomaterials: Synthesis and applications. in *Materials Today: Proceedings* vol. 18 2182–2190 (Elsevier Ltd, 2019).
78. Saleh, T. A. Nanomaterials: Classification, properties, and environmental toxicities. *Environmental Technology and Innovation* vol. 20 (2020).
79. Gong, M., Zhang, L. & Wan, P. Polymer nanocomposite meshes for flexible electronic devices. *Progress in Polymer Science* 107, 101279 (2020).
80. Mamidi, N., Romo, I. L., Leija Gutiérrez, H. M., Barrera, E. v. & Elías-Zúñiga, A. Development of forcespun fiber-aligned scaffolds from gelatin-zein composites for potential use in tissue engineering and drug release. *MRS Communications* 8, 885–892 (2018).
81. Zaarour, B., Zhu, L., Huang, C. & Jin, X. Enhanced piezoelectric properties of randomly oriented and aligned electrospun PVDF fibers by regulating the surface morphology. *Journal of Applied Polymer Science* 136, (2019).
82. Ali, F., Raza, W., Li, X., Gul, H. & Kim, K. H. Piezoelectric energy harvesters for biomedical applications. *Nano Energy* 57, 879–902 (2019).
83. Arab Hassani, F. *et al.* Smart materials for smart healthcare– moving from sensors and actuators to self-sustained nanoenergy nanosystems. *Smart Materials in Medicine* 1, 92–124 (2020).
84. Ghoshal, A., Ayers, J., Gurvich, M., Urban, M. & Bordick, N. Experimental investigations in embedded sensing of composite components in aerospace vehicles. *Composites Part B: Engineering* 71, 52–62 (2015).

85. Mahanty, B., Maity, K., Sarkar, S. & Mandal, D. *Human Skin Interactive Self-powered Piezoelectric e-skin Based on PVDF/MWCNT Electrospun Nanofibers for Non-invasive Health Care Monitoring. Materials Today: Proceedings* vol. 21 [www.sciencedirect.com](http://www.sciencedirect.com)[www.materialstoday.com/proceedings](http://www.materialstoday.com/proceedings) (2020).
86. Salehi, H., Burgueño, R., Chakrabarty, S., Lajnef, N. & Alavi, A. H. A comprehensive review of self-powered sensors in civil infrastructure: State-of-the-art and future research trends. *Engineering Structures* 234, (2021).
87. Sharma, S., Kiran, R., Azad, P. & Vaish, R. A review of piezoelectric energy harvesting tiles: Available designs and future perspective. *Energy Conversion and Management* vol. 254 (2022).
88. Pan, H. H. & Guan, J. C. Stress and strain behavior monitoring of concrete through electromechanical impedance using piezoelectric cement sensor and PZT sensor. *Construction and Building Materials* 324, (2022).
89. Chen, C., Sharafi, A. & Sun, J. Q. A high density piezoelectric energy harvesting device from highway traffic – Design analysis and laboratory validation. *Applied Energy* 269, (2020).
90. Ganesh, R. J., Shanmugam, D. B., Munusamy, S. & Karthikeyan, T. Experimental study on footstep power generation system using piezoelectric sensor. in *Materials Today: Proceedings* vol. 45 1633–1637 (Elsevier Ltd, 2021).
91. Askari, H., Khajepour, A., Khamesee, M. B. & Wang, Z. L. Embedded self-powered sensing systems for smart vehicles and intelligent transportation. *Nano Energy* 66, 104103 (2019).
92. Mouapi, A., Hakem, N., Delisle, G. Y. & Kandil, N. A novel piezoelectric micro-generator to power Wireless Sensors Networks in vehicles. in *2015 IEEE 15th International Conference on Environment and Electrical Engineering, IEEEIC 2015 - Conference Proceedings* 1089–1092 (Institute of Electrical and Electronics Engineers Inc., 2015). doi:10.1109/IEEEIC.2015.7165317.
93. Li, Z. *et al.* Harnessing energy from suspension systems of oceanic vehicles with high-performance piezoelectric generators. *Energy* 228, (2021).
94. de Pasquale, G., Somà, A. & Fraccarollo, F. Piezoelectric energy harvesting for autonomous sensors network on safety-improved railway vehicles. *Proceedings of the Institution of Mechanical Engineers, Part C: Journal of Mechanical Engineering Science* 226, 1107–1117 (2012).
95. Khazaei, M., Rezaniakolaie, A., Moosavian, A. & Rosendahl, L. A novel method for autonomous remote condition monitoring of rotating machines using piezoelectric energy harvesting approach. *Sensors and Actuators, A: Physical* 295, 37–50 (2019).
96. Nguyen, V.-C. *et al.* Printing smart coating of piezoelectric composite for application in condition monitoring of bearings. *Materials & Design* 215, 110529 (2022).

97. Deng, W. *et al.* Cowpea-structured PVDF/ZnO nanofibers based flexible self-powered piezoelectric bending motion sensor towards remote control of gestures. *Nano Energy* 55, 516–525 (2019).
98. Lazarević, Z. *et al.* *Characterization of Barium Titanate Ceramic Powders by Raman Spectroscopy*. vol. 115 (2009).
99. Sabry, R. S. & Hussein, A. D. PVDF: ZnO/BaTiO<sub>3</sub> as high out-put piezoelectric nanogenerator. *Polymer Testing* 79, (2019).
100. Zhao, M., Fu, Q., Hou, Y., Luo, L. & Li, W. BaTiO<sub>3</sub>/MWNTs/Polyvinylidene Fluoride Ternary Dielectric Composites with Excellent Dielectric Property, High Breakdown Strength, and High-Energy Storage Density. *ACS Omega* 4, 1000–1006 (2019).
101. Rubaiya, F., Mohan, S., Srivastava, B. B., Vasquez, H. & Lozano, K. Piezoelectric properties of PVDF-Zn<sub>2</sub>GeO<sub>4</sub> fine fiber mats. *Energies (Basel)* 14, (2021).
102. Ouyang, Z. W., Chen, E. C. & Wu, T. M. Thermal stability and magnetic properties of polyvinylidene fluoride/magnetite nanocomposites. *Materials* 8, 4553–4564 (2015).

## **Curriculum Vitae**

Renato Wenceslao Aguirre Corona was born in Saltillo, Coahuila, México on 21, 1994. He earned the Mechatronic Engineering degree from the University of La Salle, Saltillo Campus in December 2017. He made his internship in the industrial sector in the company BorgWarner where he fulfilled with the activities of a control technician and made analysis of the efficiency metrics for 1 year. He traveled and lived in New Zealand for 4 months to study and practice the English language. Then he returned and worked in the industrial sector over 1 year 7 months in the company BorgWarner as a Maintenance Technician for 1 year 4 months and then promoted to Maintenance Team Leader for three months. He was accepted in the Master graduate program in Nanotechnology in 2020.

This document was typed in using Microsoft Word by Renato Wenceslao Aguirre Corona